Chemistry and Physics of Solid Surfaces

Volume II

Editor

Ralf Vanselow

Associate Professor
Department of Chemistry
and
Laboratory for Surface Studies
University of Wisconsin
Milwaukee, Wisconsin

CRC PRESS, INC.
Boca Raton, Florida 33431

Library of Congress Cataloging in Publication Data

Main entry under title:

Chemistry and physics of solid surfaces.

At head of title: CRC.
Includes bibliographical references and indexes.
1. Surface chemistry. 2. Solid state chemistry.
I. Vanselow, Ralf. II. Chemical
Rubber Company. Cleveland.
QD508.C48 541'.3453 77-25890
ISBN 0-8493-0125-4 (Volume I)
ISBN 0-8493-0126-2 (Volume II)

This book originally appeared in Volume I, Issues 2, 3, and 4 and Volume 8, Issues 1 and 2 of *CRC Critical Reviews in Solid State and Materials Sciences*, a journal published by CRC Press, Inc.

International Standard Book Number 0-8493-0126-2

Library of Congress Card Number 77-25890
Printed in the United States

THEORY OF INDIRECT INTERACTION BETWEEN CHEMISORBED ATOMS

Author: **Theodore L. Einstein**
Department of Physics and Astronomy
University of Maryland
College Park, Maryland

TABLE OF CONTENTS

I. INTRODUCTION

Progress in the development of the theory of two chemisorbed atoms has been hindered by the very low symmetry of the problem. Monolayers of adatoms are simplest since they have the full two-dimensional symmetry of the substrate. Going to a (2×1) or a (2×2) adlayer, which doubles the size of the surface primitive cell, quadruples the size of a secular matrix,

raising computer time even more. At the other end of the scale, a single adatom (in a symmetric site) will at least have the point symmetry of the substrate. With jellium as a substrate, this increases to full rotational and translational symmetry. Conserved quantities ("good quantum numbers"), which make calculations simpler, are associated with these symmetries. As a result, a variety of elaborate many-body techniques have been successfully applied to these systems; there are several excellent recent reviews.[1,2] For two adatoms on a surface, there is little or no symmetry, typically just a twofold rotation or mirror plane (often leading to splittings of levels).

This review will explore the many chemisorption-induced ways by which two atoms can interact, with special emphasis on the indirect electronic ["pair"] interaction between light gas or transition series atoms on a [transition] metal. Since experimental data on these systems appear in the papers preceding and following this one, we will concentrate on theory here. Progress in the field has come in the form of study of self-consistency and correlation effects (which seem to be less important than might be expected) and multiparameter-model attempts to describe real systems. Next, we shall show in a single simple model how pair, three-adatom, etc. interactions combine to produce ordered overlayers. We will briefly consider changes in density of states (DOS) caused by two-adatom interactions from a similar viewpoint and also show the more dramatic effects that arise when these combine to produce an ordered overlayer. Finally, we shall introduce temperature into the problem, discuss how chemisorption systems can be among the best examples in nature of a lattice gas, and consider disordering transitions and island shapes, complementing the previous paper. In closing, we shall speculate on areas ripe for development. An appended note considers the asymptotic nature of the pair interaction.

II. PAIR INDIRECT INTERACTION ENERGIES

A. Fundamental Orientation

If chemisorbed atoms are sufficiently close to overlap each other, there will be a strong direct interaction. This interaction is essentially a chemical bond, comparable in strength to the chemisorption bond. For a larger interadatom distance R, the interaction falls off exponentially along with the overlap so that it is negligible for R more than a few angstroms. Most of the physics of this problem comes from the two adatoms and their substrate nearest neighbors; hence, a cluster calculation is appropriate. These interactions are important for supersaturated or even monolayer-covered surfaces. They also arise in the problem of dissociation and reassociation of adsorbing molecules (e.g., the question of whether there is an activation barrier), which has been studied both schematically[3] and in great detail.[4]

If the chemisorption bond is polar, substantial electric dipoles will arise. Kohn and Lau[5] recently showed that the nonoscillatory part of the dipole-dipole interaction energy on metals goes as $2\,\mu_a\,\mu_b/R^3$ for large R. The novel factor of 2 comes essentially from the fact that although outside a metal the image charge acts as though it were at the image point, it in fact lies on the surface. Hence, the dipole exerts a force on an incoming second charge that is twice what it would in vacuum. Inserting numbers, we find this interaction energy to be 1.25 eV ~~625 meV~~ times the two dipoles in debyes over R^3 in angstroms.

Two adatoms will always attract each other weakly via the van der Waals' interaction.[6] The leading term is the dipole-dipole contribution, which goes as $-C/R^6$; C in turn is proportional to the square of the polarizability; is roughly 30 eV-Å^6 for Ar, N_2, and O_2; and is five times as great for Xe.[6a] For physisorbed gases, this mechanism dominates the interaction; hence, the details of the interatomic potential have been studied extensively. To fit gas-phase data, one must go beyond a simple R^{-12} Lennard-Jones repulsion (to some exponential description) to avoid overestimating C by nearly a factor of two.[6a,6c] Two higher order gas-phase effects are nonnegligible: (1) The R^{-8} dipole-quadrupole force which increases the depth of the well minimum by roughly 10%[6b,6c] and (2) the repulsive (in all important cases) R^{-9} triple-dipole (Axilrod-Teller) interaction, the magnitude of which is at most 3% (for Ar) to 5% (for Xe) of a pair interaction (with all distances set at the separation giving the well minimum).[6c,6d] A variety of calculations of rare gas adsorption

onto jellium,[6e] continuous dielectrics,[6f] Xe crystals,[6g] and graphite[6h] all show that physisorption reduces the gas-phase pair attraction by roughly 20%. To apply these results to chemisorption, we can invoke surface molecule picture to posit that the van der Waals' interaction between, say, two chemisorbed O atoms is similar to that between two O_2 molecules (although now the molecules are oriented), i.e., roughly -25 eV-Å^6/(R[Å]).[6] At second- and third-neighbor separations on Ni(001), for example, this yields an interaction of -13 and -2 meV, respectively, which is usually negligible compared to the electronic indirect interaction. For heavy adsorbates (e.g., W or Re) these numbers could be several times greater;[6a,6j] no firm data exist.

The preceding interactions have been classed as "through space", in distinction to "through bond"[7] or indirect interactions, which are dominated by bonding to the background. The essence of this interaction is seen in Figure 1, taken from Grimley's pioneering work[8] on this problem. Consider two atoms, each with an atomic potential producing some [relatively high-lying] bound state. In free space (and at moderate separation), each of the bound-state wave functions will remain confined near its atomic site; vacuum barrier is insurmountable. If, alternatively, they are adsorbed onto (or absorbed into) a metal, both atomic wave functions can tunnel through the narrow potential barrier to the metal and couple with metal wave functions. Figure 1B shows how both atomic wave functions might couple to one such background eigenstate. If the coupling places the two atomic wave functions in (out of) phase, the interaction is attractive (repulsive), lowering (raising) the energy of the participants. From the oscillatory nature of the intermediate wave function, the electronic indirect interaction should be oscillatory in sign as a function of interadatom distance. It should be isotropic in orientation if and only if the metal background is. In fact, there is a quasicontinuum of states via which the two atomic orbitals can couple. As distance increases, fewer will match well with the atomic orbitals, causing a rapid decay with separation.

Analysis of this pair problem generally proceeds from a two-impurity Anderson-type model:[9,10]

$$H = H_{\text{metal}} + H_a + H_b + H_{am} + H_{bm} \tag{1}$$

Here, H_{metal} is the Hamiltonian for the unperturbed metal, H_a and H_b for the isolated impurity atoms, and H_{am} and H_{bm} the coupling between atoms and metal. The absence of H_{ab} indicates that there is no direct interaction.[10] Work on the problem has amounted to taking progressively more realistic expressions for some of these terms and solving the resulting system to varying levels of approximation. We shall follow the common practice of assuming that atoms a and b are identical. The above ansatz is couched in an atomic orbital picture, at least for the two adatoms. It will be shown that this framework is well suited to our problem, although it does neglect orbital deformation effects and related phenomena.

For substrates, typically

$$H_{\text{metal}} = \sum_{\underline{k}\mu\sigma} e_{\underline{k}}^{\mu} n_{\underline{k}\sigma}^{\mu} \tag{2}$$

thereby assuming a one-electron description; μ is a band index, which is dropped in single-band models. Occasionally many-body effects are considered in a Hubbard model sense.[11,12] Since only lateral crystal momentum $\underline{k}_{\parallel}$ is conserved for a slab or semi-infinite crystal, $\underline{k}$ merely labels the states in some suggestive fashion.

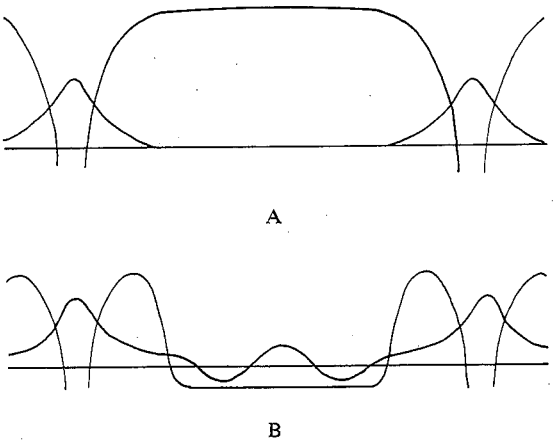

FIGURE 1. Schematic of the pair interaction. Wave functions for two atoms moderately separated (A) in vacuum and (B) chemisorbed on a metal. (From Grimley, T. B., *Proc. Phys. Soc.* (London), 90, 751, 1967. With permission.)

The coupling between atom and host has the Anderson form

$$\mathcal{H}_{am} = \sum_{\underline{k}\sigma} \left[V_{ak}\, c_{a\sigma}^{+}\, c_{\underline{k}\sigma} + \text{h.c.} \right] \tag{3}$$

with b simply replacing a in $\mathcal{H}_{bm}$. Except in the most detailed band-type calculation, one assumes that the only k dependence in V_{ak} comes from its position, so that in a position representation

$$\mathcal{H}_{am} = -V \sum_{\sigma} \left[c_{a\sigma}^{+}\, c_{o\sigma} + \text{h.c.} \right] \tag{4}$$

for binding to a single site or position (called o) or for binding to some group orbital $\sum_i \alpha_i \phi_i(r)$ [with $\sum_i \alpha_i = 1$],

$$\mathcal{H}_{am} = -V \sum_{i\sigma} \left[\alpha_i\, c_{a\sigma}^{+}\, c_{i\sigma} + \text{h.c.} \right] \tag{5}$$

In this case, the group summation may be included either in the coupling[13,14] or in the metal part.[15,16] In principle, this coupling should also consider an overlap term between atoms and metal. Numerous detailed articles[12,17-20] have addressed this question. The usual result is to "renormalize" previously stipulated natural orbitals (and resulting energies) with Löwdin[21] or Gram-Schmidt[22] schemes.

The adatom part of the Hamiltonian is

$$\mathcal{H}_a = \epsilon_a^{\circ} \sum_{\sigma} n_{a\sigma} + U\, n_{a\uparrow}\, n_{a\downarrow} \tag{6}$$

and similarly for $\mathcal{H}_b$. This expression can be generalized to include degenerate orbitals,[23] multiple levels, etc. Most simply, one might parametrize ε_a° as the ionization level of the adatom and U as the difference between it and the affinity level. ε_a° should be raised and U reduced by consideration of correlation effects (screening and image charges).[24] In a [restricted] Hartree-Fock sense, we can neglect U entirely and replace ε_a° by $\varepsilon_a = \varepsilon_a^{\circ} + U\langle n_{a\sigma}\rangle$, where $\langle n_{a\sigma}\rangle$ is the mean occupation of the adatom for either spin direction. For neutral chemisorption, $\langle n_{a\sigma}\rangle$ is 1/2, suggesting that ε_a be the [negative] average of the ionization and affinity energies, as in many chemical molecular orbital calculations.[25] Pandey[26] has used the idea of chemical transferability: he adjusts the adatom and coupling parameters so that cluster computations of small molecules made of the relevant elements fit the levels found in photoemission experiments; presumably, the same parameters carry over to the chemisorption system. Brenig and Schönhammer,[27] Hertz and Handler,[28] and Bell and Madhukar[29] have taken steps beyond Hartree-Fock in the case of single-atom adsorption. The first group[12] has also shown in the pair problem that self-consistency effects are relatively unimportant, compared to the single atom case, as will be discussed below.

To obtain the quantities of interest — interaction energy and change in density of states (DOS) — it is helpful to first compute the phase shift

$$\eta(\epsilon) = \text{Im ln det}\,(1 - G(\epsilon)\hat{V}) \tag{7}$$

where $G(\varepsilon)$ is the advanced Green's function for the unperturbed system (in this case $\mathcal{H}_{metal} + \mathcal{H}_a + \mathcal{H}_b$) and V is the perturbing potential (here the chemisorption coupling $\mathcal{H}_{am} + \mathcal{H}_{bm}$. This approach makes optimal use of the symmetry of the unperturbed system. In terms of η, one finds the change in DOS to be

$$\Delta\rho\,(\epsilon) = \pi^{-1}\,(\partial/\partial\,\epsilon)\,\eta(\epsilon) \tag{8}$$

and the interaction energy

$$2 \int_{-\infty}^{\epsilon_F} (\epsilon - \epsilon_F)\,\Delta\rho\,(\epsilon)\,d\epsilon$$

$$= -\frac{2}{\pi} \int_{-\infty}^{\epsilon_F} \eta(\epsilon)\,d\epsilon \tag{9}$$

where the factor of 2 comes from spin degeneracy and the use of $\varepsilon - \varepsilon_F$ rather than just ε indicates that the number of electrons rather than ε_F is being fixed.[8,15,30]

To evaluate the phase shift in this framework, the adatom sites (a and b) are written first, then the substrate nearest neighbors to which they couple (o and n), and finally all other substrate sites. The matrix $(1 - G\hat{V})$ then differs from a unit matrix only in the upper left-hand 4 × 4 block:

$$\det(1 - \hat{GV}) = \det \begin{bmatrix} 1 & 0 & -G_{aa} V_{ao} & 0 \\ 0 & 1 & 0 & -G_{bb} V_{bn} \\ -G_{oo} V_{oa} & -G_{on} V_{nb} & 1 & 0 \\ -G_{no} V_{oa} & -G_{nn} V_{nb} & 0 & 1 \end{bmatrix} \quad (10)$$

Although this expression implicitly assumes that the adatoms sit in the atop position, it can be easily generalized by modifying the G_{ij} (i,j = o,n) to represent a hybrid of substrate orbitals.[16] While this determinant can be evaluated straightforwardly by expansion in minors, this is not so for the three-adatom case to be considered later. Using row reduction techniques, Equation 10 can be rewritten as

$$\det(1 - \hat{GV}) = \det \begin{bmatrix} 1 - G_{aa} V_{ao} G_{oo} V_{oa} & -G_{aa} V_{ao} G_{on} V_{nb} & 0 & 0 \\ -G_{bb} V_{bn} G_{no} V_{oa} & 1 - G_{bb} V_{bn} G_{nn} V_{nb} & 0 & 0 \\ -G_{oo} V_{oa} & -G_{on} V_{nb} & 1 & 0 \\ -G_{no} V_{oo} & -G_{nn} V_{nb} & 0 & 1 \end{bmatrix} \quad (11)$$

so that the nontrivial part is isolated in the upper left 2 × 2 matrix, taking full advantage of the locality of the perturbation. For identical adatoms, all $\hat{V}$ elements are $-V$, $G_{bb} = G_{aa}$, $G_{nn} = G_{oo}$, and $G_{no} = G_{on}$, yielding

$$\eta = \mathrm{Im} \ln \left| (1 - V^2 G_{aa} G_{oo})^2 (1 - V^4 G_{on}^2 \bar{G}_{aa}^2) \right| \quad (12)$$

where $\bar{G}_{aa} = G_{aa}/(1 - V^2 G_{aa} G_{oo})$ is a renormalized Green's function for the adatom due to single-atom adsorption. Because of the logarithm, the phase shift (and hence the changes in DOS and energy) characterizing the "pair" interaction of the adatoms can be obtained directly from the phase shift associated with $(1 - V^4 G^2 \bar{G}^2)$,[15] rather than from explicitly subtracting twice the single-adatom phase shift from the two-adatom shift.[12] For any number of adatoms, the single-adatom adsorption part factors out of the matrix.[15,31] On the other hand, as will be seen, for more than two adatoms there is no way to factor out the pair effects from the higher order ones.[32]

B. Basics of the Electronic Indirect Interaction

In the LCAO framework, the formula for the pair interaction energy E_n between the adatoms adsorbed on sites o and n (which we identify as nth nearest neighbor sites on the surface) is, from Equations 9 and 12,

$$E_n = -\frac{2}{\pi} \int_{-\infty}^{\epsilon_F} \mathrm{Im} \ln \left[1 - V^4 G_{on}^2 \bar{G}_{aa}^2 \right] d\epsilon \quad (13)$$

Later, we shall refer to the interacting pair itself by E_n, in a manner that should cause no confusion. This nth-neighbor pair interaction is an implicit function of ϵ_F and V as well as the binding site symmetry.

To understand this interaction, we first expand the logarithm and consider the lowest order term[33] (often a good approximation)

$$E_n \sim \frac{2}{\pi} \int_{-\infty}^{\epsilon_F} \mathrm{Im}\, V^4 G_{on}^2(\epsilon) \bar{G}_{aa}^2(\epsilon) d\epsilon \quad (14)$$

If $\bar{G}_{aa}$ is neglected, Equation 14 is just the RKKY interaction energy,[34] in which two localized spins interact via coupling to a bulk conduction electron sea. Hence, the propagator $G_{on}(\epsilon)$ — or more precisely $G(R;\epsilon)$ — is that for jellium, making the interaction isotropic. The energy is proportional to $F(x) \equiv (x \cos x - \sin x)/x^4$, where x is $2k_F R$ and R is the distance between the spins. It is thus oscillatory in R and drops off asymptotically as R^{-3}, characteristic of Fermi surface domination.

Grimley[8,31] was the first to apply the Anderson model to chemisorption. In then-standard fashion, he neglected the detailed energy dependence of G_{oo} and G_{on}, making what amounts to the weak-binding approximation of replacing them by their values at resonance. He reports analytic results in several limits, using as a substrate a semi-infinite single-band crystal with a phenomenological surface reactivity. Under particular conditions, he evaluates the asymptotic form of the pair interaction energy and

finds it to vary sinusoidally and decay as R^{-3}, except in "critical directions" where it falls as R^{-5}.[31,114] [A critical direction was defined to lie in the surface plane perpendicular to $\vec{\tau}$, where $\vec{\tau}$ is the third primitive vector of the substrate, the first two being taken in the surface plane.] Recent clarifying results are presented in the appended note.

Extensive calculations of pair interactions were performed by Einstein and Schrieffer[15] on a system in which the adatoms and coupling are much like Grimley's but in which the substrate is the {100} face of a single-band simple cubic crystal (cubium).[35] No approximations beyond the tight-binding model itself are made in the actual calculation. Table 1 capsulizes the results. The energies are measured in units of one-sixth of the bandwidth (i.e., the substrate tight binding nearest-neighbor hopping is $-1/2$ in these units). For the typical transition metal d-band being modeled, this unit is of the order of 1 to 2 eV. The Fermi energy and the energy ε_a representing the principal interacting orbital of the adatom level are measured relative to the center of the band. As Table 1 illustrates, the pair interaction is highly anisotropic, oscillatory in sign, and rapidly decaying. At close separations, the decay is precipitous and more exponential than inverse power-like, dropping roughly by 1/5 with each lattice spacing. A laborious calculation[19] (see the appended note) verifies Grimley's prediction of R^{-5} behavior asymptotically — every direction on the {100} face of cubium is critical. The change from exponential to inverse power dependence corresponds to many electronic states participating in the pair interaction vs. just the Fermi surface electrons (as in RKKY) doing so in the asymptotic limit. The energies are very sensitive to the adatom binding site. They are comparatively insensitive to changes in ε_a and V and are somewhat more sensitive to shifts in the Fermi energy, especially for larger interadatom separation. Typical values of the magnitude of the nearest, next-nearest, and third-nearest pair energies are 1×10^{-1}, 2×10^{-2}, and 8×10^{-3} units, although each can vary over a range of an order of magnitude.

C. Coulombic Effects: Self-consistency and Correlation

Questions of self-consistency have pervaded most recent efforts in the pair problem. In the LCAO framework, since the electron orbitals are fixed at the outset, self-consistency is discussed in terms of the Friedel sum rule[36] (which in this case requires charge neutrality within some finite range of an adatom) rather than Poisson's equation.[2] Typically, ε_a is manipulated[37-39] (making it a derived rather than a free parameter). Often, a similar term is added to the nearest neighbor(s) on the surface,[37,38] thereby inviting new surface states.[35,40] Sometimes, off-diagonal Coulomb terms are also included in various ways.[38,39] Generally, neutrality is required either at each site[37,38] or just in the surface cluster consisting of the adatom and its nearest neighbor(s),[14,37] excluding any longer range oscillations. The quantitative results are rarely compelling. Qualitatively, one finds[16a] the following results for a less-than-half-filled band (the opposite being true for more than half filled): ε_a will move toward the center of the band to reduce the charge that would tend to accumulate near the chemisorption band; a diagonal term would do the same on the substrate neighbor, except that it should have originally been negative to compensate for the band narrowing due to cleaving the crystal.

A second approach assumes that in a strongly chemisorbed system, the physics of the pair interaction lies in a surface molecule. A small cluster is treated carefully, gaining an improved description of local Coulomb effects at the expense of any background effects from the substrate. From studies of W_2H and W_3H_2, for example, Grimley and Torrini[41] conclude that H atoms at nearest-neighbor sites on an W{100} will be unstable, with the repulsive energy being on the order of 200 meV. (Interestingly, the repulsion was twice as great in an Anderson model[9] description as in a Hubbard model.[11]) This method is not very appropriate for more widely separated pairs, since the distance from the adatom to the edge of the cluster should presumably be at least the distance from the other adatom. Since the "substrate" wave functions on which the pair effects hinge are sensitive to the details of the cluster, matching-conditions to the outside must be delicately tuned. Moreover, in cases where adatoms bond to a common substrate atom, some anomalous structure may arise[15] which should not be generalized. The best hope for cluster approaches is to embed them in exactly solvable semi-infi-

TABLE I

Display of the Pair Interaction Energy E_n Suggesting the Sensitivity of Adatom Arrays to Changes in the Fermi Level, the Hopping Potential, the Adatom Energy Level, and the Binding Site Symmetry

	Binding site														
	A			C						B			BP		
	3	4	5	3	4	5				3	4	5	3	4	5
	1	2	4	1	2	4				1	2	4	1	2	4
n =	0	1	3	0	1	3	6	9	13	0	1	3	0	1	3
$\varepsilon_F = 1.2$	−7.7	−7.5	+7.5	−8.3	+7.1	−7.4				+8.4	+8.3	−6.1	−7.9	−7.4	−6.1
$\varepsilon_a = -0.3$	+8.9	−8.1	−7.5	−9.0	−8.0	+7.1				−9.3	−8.4	+8.3	+8.2	−8.4	−7.4
V = 3/2	0	+8.9	−7.7	0	−9.0	−8.3	−6.6	+6.1	+4.6	0	−9.3	+8.4	0	+8.2	−7.9
	c (2 × 2)					(1 × 1)					(1 × 1)			c (2 × 2)	
$\varepsilon_F = 1.2$	−7.8	−6.7	+7.4	−8.6	−6.2	−7.8				+8.7	+8.1	−7.6	+7.6	+7.0	−7.6
→ $\varepsilon_a = 0.0$	+8.8	−8.4	−6.7	−9.4	−8.6	−6.2				−9.3	−8.3	+8.1	+9.0	−8.3	+7.0
V = 3/2	0	+8.8	−7.8	0	−9.4	−8.6	+7.7	−5.8	+5.3	0	−9.3	+8.7	0	+9.0	+7.6
	c (2 × 2)					(1 × 1)					(1 × 1)			c (2 × 2)	
$\varepsilon_F = 1.2$	−7.7	+7.7	+6.9	+8.5	−7.5	+7.8				+8.5	−7.9	−7.8	−7.8	+6.9	−7.8
$\varepsilon_a = -0.3$	+8.6	−8.6	+7.7	−9.3	−8.4	−7.5				−9.1	+7.5	−7.9	+9.1	+7.5	+6.9
→V = 2	0	+8.6	−7.7	0	−9.3	+8.5	+7.6	−6.1	+4.9	0	−9.1	+8.5	0	+9.1	−7.8
	c (2 × 2)					(1 × 1)					(1 × 1)			(2 × 2)	
→ $\varepsilon_F = 0.9$	−7.5	+7.7	−7.0	+8.1	−7.9	+7.7				+8.4	−7.7	−7.7	+6.3	+7.8	−7.7
$\varepsilon_a = -0.3$	+8.5	−8.5	+7.7	−9.3	−8.4	−7.9				−9.2	−7.1	−7.7	+9.0	−7.1	+7.8
V = 3/2	0	+8.5	−7.5	0	−9.3	+8.1	+7.5	−6.3	+4.7	0	−9.2	+8.4	0	+9.0	+6.3
	c (2 × 2)					(1 × 1)					(1 × 1)			c (2 × 2)	
→ $\varepsilon_F = 1.5$	−6.7	−7.8	+4.4	−7.3	+5.8	−6.8				−8.4	−7.7	+7.0	+6.7	−7.0	+7.0
$\varepsilon_a = -0.3$	+8.7	+8.3	−7.8	+6.2	−7.2	+5.8				−8.9	+6.2	−7.7	−8.7	+6.2	−7.0
V = 3/2	0	+8.7	−6.7	0	+6.2	−7.3	−6.3	+5.5	+4.5	0	−8.9	−8.4	0	−8.7	+6.7
	c (4 × 2)					c (2 × 2)					(1 × 1)			(1 × 1)	

Note: One adatom sits at the origin "0", the pair energy is for a second adatom at the n^{th} nearest-neighbor site. The magnitude of the number given is 10 plus the common logarithm of the magnitude of the interaction. A plus (minus) sign means that the interaction is repulsive (attractive). Thus, table entries of +8.9, −7.7, and −6.6 represent E_ns of $+8 \times 10^{-2}$, -5×10^{-3}, and -4×10^{-4}, respectively. The energy unit is one sixth the substrate band width, roughly 1 to 2 eV. Each chart is labeled by the symmetric adlayer pattern predicted. (From Ref. 15, with minor alterations.)

nite substrate.[1,42] Grimley and Pisani[43] have done so for clusters containing single adatoms and calculated in SCF-LCAO-MO scheme.

Schönhammer et al.[12] have carefully treated correlation effects in the pair problem. For each adatom and spin, they project onto the two atomic states in which that adatom is either occupied or unoccupied by an electron of opposite spin. Since they focus on the adatoms, they calculate interaction energies using an expression which requires only the [perturbed] Green's function on the adatoms, G_{aa}.[44] For the interaction of a single adatom, this expression is

$$E_{single} = \frac{1}{2\pi i} \oint_C \mathrm{Tr} \{(z + \epsilon_a^0 + \Gamma(z) - 2z\Gamma'(z)) G_{aa}(z)\} dz - \epsilon_a^0 \quad (15)$$

The trace runs over the four possible adsorbate atomic states; the contour encloses the occupied energy states in the complex energy plane (i.e., $\frac{1}{2\pi i} \oint_c$ corresponds to $\int_{\infty}^{\epsilon_F}$). $\Gamma(z)$ is a one-body self-energy analogous to $V^2 G_{\infty}$. Since the projected field operators do not satisfy the canonical anticommutation relations, Schönhammer et al.[12] invoke an equation of motion approach.[45] They arrive at a (2 × 2) self-energy matrix M in the space of atomic states of one spin. M is expressed in terms of Γ and the many-body contribution m(z), which is the source of mixing of the atomic levels and is calculated to order V^2 either in some limiting case[27,46] or variationally.[12] In the two-adsorbate case, a generalized form of Equation 15 is written, but to find the pair interaction, twice E_{single} of Equation 15 must be subtracted; there is no natural factorization as in Equation 12. The self-energy matrix M now becomes (4 × 4), having components for each adatom. A new variational parameter is introduced which (for weak V) reduces to the expectation value of the dot product of the spins on the two adatoms (which leads to small splittings between ferromagnetic and antiferromagnetic spin configurations). Formal results of Schönhammer et al.[12] are capable of also including scattering in the substrate and a direct interaction between the adatoms (that being a simple hopping term),[10] although their numerical work neglects these possibilities. Using a {100} cubium substrate with parameters appropriate to H on Ni, Schönhammer[47] had previously shown from a variational approach that the single-adatom binding energy is roughly one-third stronger than in Hartree-Fock (although the two curves did have the same structureless shape — a U with flared verticals — as a function of ϵ_F). As shown in Figure 2, Schönhammer et al.[12] find that this correlation energy, one-fourth the binding energy, roughly cancels out when the

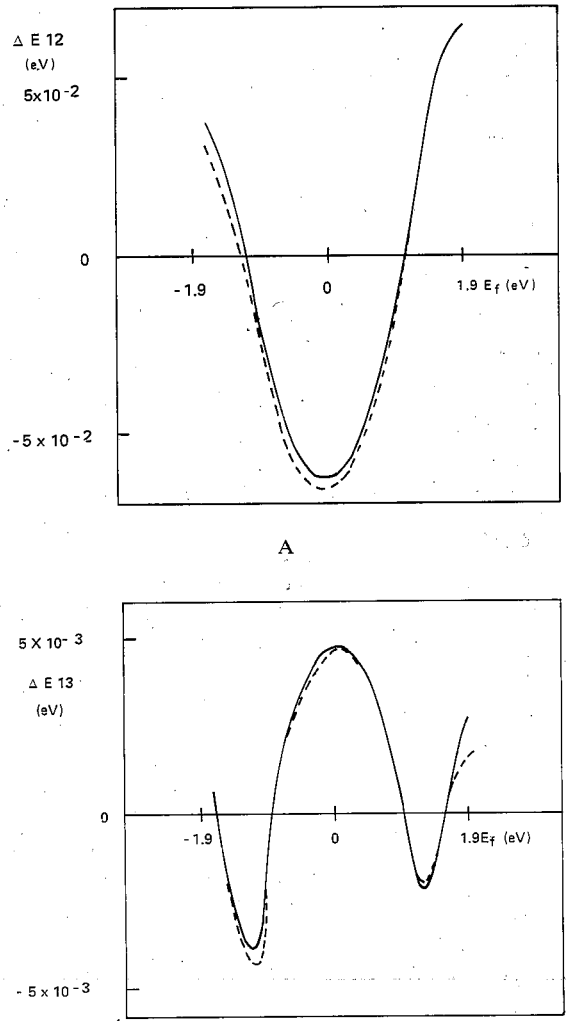

FIGURE 2. Pair indirect interaction energy for two Hs in the atop position at (A) <10> nearest ("ΔE_{12}," called E_1 in text) and (B) next-nearest ("ΔE_{13}," our E_3) neighbor sites on cubium, plotted vs. Fermi energy (with other parameters appropriate to Ni). The dashed curves are Hartree-Fock; the solid curves also include correlation as treated by Schönhammer et al.[12] (From Schönhammer, K., Hartung, V., and Brenig, W., *Z. Phys. B*, 22, 143, 1975. With permission.)

pair interaction energy is computed. Although this cancellation is reported to be less complete for other parameters, the qualitative behavior holds for V's on the order of the critical hopping (below which Hartree-Fock local moments arise). In addition to confirming the anisotropic, oscillatory behavior of the pair interaction, these authors corroborate the roughly exponential fall-off with separation (for interadatom distances of order one to four lattice constants). The implication of this work is that correlation effects (in the form of careful treatments of the Anderson Coulomb term), while important for single-adatom effects, can (to a reasonable approximation) be neglected in computing pair (and higher order) effects.

D. Semirealistic Calculations

Recent research in chemisorption theory has stressed generation of numerical results to quantitatively fit data from UV photoemission, ion neutralization spectroscopy, and low-energy electron diffraction (LEED) experiments. The primary object has been to compute the spatial and energy distribution of the electron density near the surface region and to find exact locations of surface states. For these applications, self-consistency (here, in a Poisson's equation sense) is crucial. To gauge the role of such effects, much work has been done on the adsorption of single adatoms on jellium.[48] Meanwhile, realistic self-consistent pseudopotential substrate calculations began appearing[2] with Appelbaum and Hamann's[49] treatment of Na{100} and Si{111} and followed by many other studies[50] of crystalline semiconductors and simple metals. Pair interactions on these substrates are undramatic. On alkalis (aside from the fact that they are weak chemisorbers), adsorption will involve so much charge transfer that the dipole-dipole repulsion dominates lateral interactions. Since semiconductor electrons are relatively localized in covalent bands, it is difficult to propagate electrons from one adsorption site to another, as manifested by the band gap. For most of the schemes cited above, consideration of anything but a (1 × 1) overlayer is prohibitive. Pandey's[26] multiparameter tight-binding approach for H on Si{111} and Ge{111} could presumably be directed toward the two-adatom problem. Tosatti[51] has considered the interaction between adatom pairs on Si{100} 2 × 1, assuming a short-range defect potential for the adatoms and linear response by the surface electrons. His pair interaction is always repulsive and oscillatory (in strength) with separation, but with an exponentially decaying envelope (due to trying to propagate electrons in the gap).

Realistic calculations for transition and noble metals are now appearing. Terakura[52] and Davenport et al.[53] (who did a semi-infinite substrate) considered Ni{100} in a nearest neighbor LCAO tight-binding model. Kasowski[54] applied the LCMTO (linear combination of muffin-tin orbitals) to this substrate, then added (1 × 1) overlayers of O and Na to study adlayer-induced surface states for (2 × 2) overlayers [rationalizing that the states are basically one-adatom effects]. Promising non-self-consistent calculations have been done for Cu films using multiple-scattering[55] and LCMTO[56] techniques and for Fe and Cu slabs of several orientations using a many-parameter tight-binding model.[57] Self-consistency has just been achieved for Cu{100} and Ni{100} films with an *ab initio* calculation[58] and for Cu{111} with an elaborate supplemented Gaussian orbital scheme in a local density approximation.[59] Since these calculations are at the border of computability, we can expect nothing beyond (1 × 1) overlayers for the near future.[58]

The most advanced multiparameter calculation of pair effects is Burke's[23] study of two transition metal adatoms on a transition metal substrate. The goal was to better understand pair data gleaned from experiments performed by Tsong and co-workers,[60,61] Bassett,[62] and Graham and Ehrlich,[63] using field ion-microscope tips (described in the subsequent paper). Generalizing Einstein and Schrieffer,[15] Burke first shows how fivefold degenerate adatoms may be incorporated into the formation starting with Equation 7 by an orbital-peeling matrix procedure. The idea is to (1) focus on one of a pair of nearby adatoms, (2) remove it from the system orbital by orbital, and (3) replant it "infinitely" far away (as though there had been originally five single-level adatoms rather than one at each site of the pair). In this procedure, the bulk is unspecified. In actual calculations, his substrate is the {100} or {110} face of a semi-infinite bcc crystal, with adatoms imagined as the same element (viz., W) as the substrate and

sitting in the otherwise vacant lattice sites above the surface. All diagonal matrix elements are set at the energy zero; the possibility of having to modify what amounts to $\varepsilon_a = 0$ is discussed and dismissed, thereby completely neglecting self-consistency corrections. Overlap is also excluded. Slater-Koster[64] matrix elements between nearest and next-nearest sites are calculated in terms of the two sets of 3 d-d tight-binding parameters. Alas, these six values are simply scaled up from narrow band values,[65] ignoring any details of hybridization with s-p electrons.[66] Computation of substrate Green's functions is not at all straightforward; Burke eventually adopts a technique which combines the continued fraction approach[67] with a scheme counting poles and zeros on the real energy axis. When the adatoms are separated by just a [bulk] nearest or next-nearest neighbor distance, a direct interaction between them can also be included, as shown in Figure 3. Here, the interaction energy is plotted as a function of substrate filling for a sample pair orientation of the {110} surface. In Figure 3A, with no direct interaction, the curve looks similar to those of Einstein and Schrieffer.[15] Inclusion of the direct interaction (Figure 3B) can make a substantial difference. Overall, Burke reconfirms that the pair interaction energy has roughly the same size as described by Einstein and Schrieffer[15] and that it oscillates as a function of ε_F for fixed separation and as a function of R for fixed ε_F. In a rather cursory look at decay with separation, Burke finds much faster fall-off on the {110} face than the {100}; there are no analytic results. The pair binding of a nearest-neighbor dimer on the {110} surface is calculated to be nearly five times the experimental value of 0.3 eV.[60-62] Another difficulty is that recent work[61] suggests that the adsorbed W sits in a "surface site" rather than a "vacant lattice site". Burke alleges that this makes little difference, but gives no supporting evidence; in light of the results of Einstein and Schrieffer[15] (see Table 1), especially the difference between the two bridge configurations, such insensitivity is surprising. In short, theory is still unable to make quantitative predictions. Burke suggests a number of sources of error, but aside from adding a Coulomb counter term or massaging parameters, it is not clear how to improve matters simply; better substrates are needed.

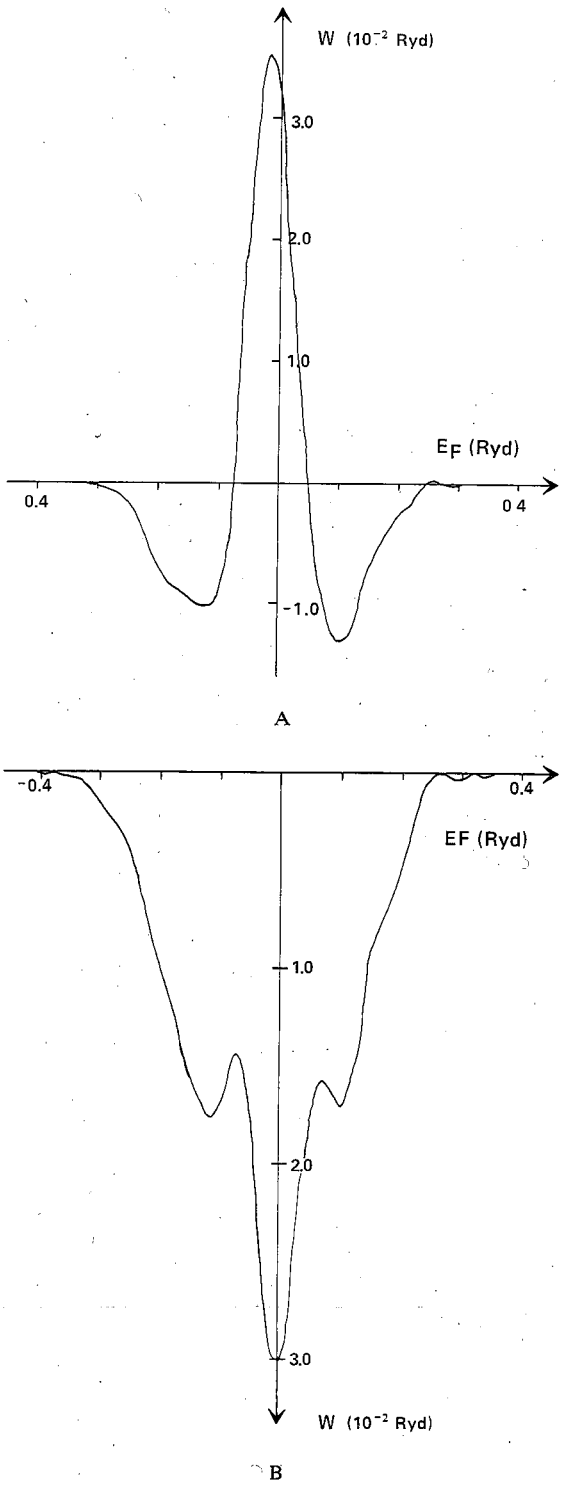

FIGURE 3. Burke's plot of pair interaction energy (called W) vs. substrate Fermi energy for two adatoms at next-nearest neighbor [above-the-surface unoccupied lattice] sites on the {110} face of a bcc crystal, with (A) direct interaction set to zero and (B) direct interaction included. (From Burke, N. R., *Surf. Sci.*, 58, 349, 1976. With permission.)

E. Lattice Indirect Interactions

Cunningham et al.[68] have studied the contribution to the free energy of the interaction between two identical adatoms via the substrate phonon field. The adatoms sit in the atop position on the {100} face of cubium. Results are computed as a function of the three dimensionless quantities: adatom mass over substrate mass, adatom-substrate coupling over substrate-substrate coupling, and interadatom separation R (in lattice constants). They find that the zero point energy is invariably attractive and that it decreases monotonically in strength with increasing R, going like R^{-7} for large R and as shown in Figure 4 for shorter R. This figure shows that the attraction is at most $10^{-4}\ \hbar\omega_L$ (where ω_L is the maximum phonon frequency) or of the order of 10^{-6} eV, and, is thus nearly always negligible. We note in passing that Schick and Campbell[69] obtain an interaction four orders of magnitude greater in a model inappropriate to chemisorption: their adatoms are delocalized and treated as Bloch waves.

Very recently, Lau and Kohn[70] investigated the long-range interaction between two adatoms due to classical elastic distortion of the substrate. For identical atoms, this interaction is always repulsive; for different adatoms, the energy can have either sign. The energy depends on the Poisson ratio and the shear modulus (inversely) of the substrate. It decays as R^{-3}, just as does the dipole-dipole repulsion, but (for xenon on noble metals) is roughly an order of magnitude smaller. On the other hand, at nearest-neighbor sites, it is three or four orders of magnitude greater than the phonon-mediated attraction just discussed; in essence the calculation of Cunningham et al.[68] gives the leading quantum correction to the classical distortive effects.

III. MULTIADATOM EFFECTS

A. Three-adatom (Trio) Interaction

Thus far, this discussion has been concerned with no more than two adatoms on the surface. Except for field-ion-microscope experiments, real situations involve large numbers of chemisorbed atoms. Einstein and Schrieffer[15] take the view that overlayer electronic energies are overwhelmingly dominated by nearest-pair interactions. Calculations of changes of DOS raised some questions about convergence, prompting many of the calculations below.

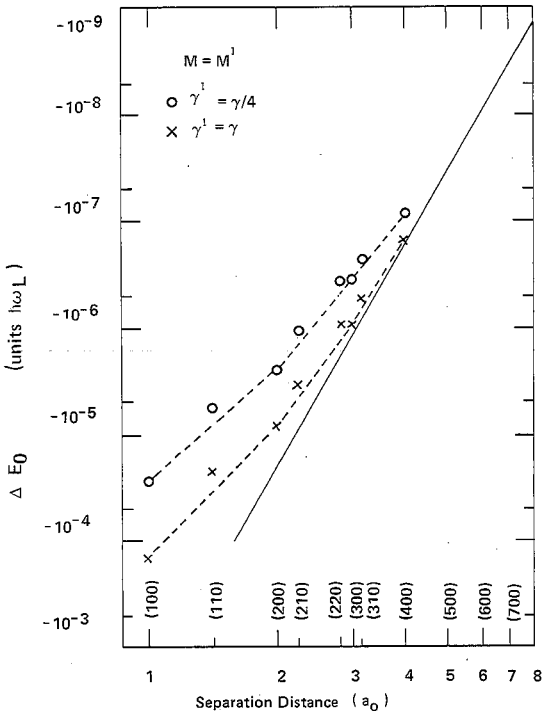

FIGURE 4. Zero point energy of the pair phonon indirect interaction as a function of separation distance for two values of the ratio γ'/γ of adatom-substrate force constant (coupling) to substrate interatomic force constant. The adatom and crystal atom masses are identical. The solid line gives the asymptotic limit, while the points are specific numerical results. (From Cunningham, S. L., Dobrzynski, L. and Maradudin, A. A., *Phys. Rev. B*, 7, 4643, 1973. With permission.)

Equation 11 was written to permit an easy generalization to three adatoms. If the sites to which the adatoms bind are lth, mth, and nth nearest neighbors, we find, making the same identifications that led to Equation 12, that

$$\eta = \mathrm{Im}\ \ln\left[(1 - V^2\ G_{oo})^3\ \Delta\right]$$

where

$$\Delta \equiv 1 - V^4\ \bar{G}_{aa}{}^2\ (G_{ol}{}^2 + G_{om}{}^2 + G_{on}{}^2) - 2V^6\ \bar{G}_{aa}{}^3\ G_{ol}\ G_{om}\ G_{on} \qquad (16)$$

As indicated in Section II.A, Δ does not factor. We define a trio interaction energy[16] as

$$E_{lmn} \equiv -\frac{2}{\pi}\int_{-\infty}^{\epsilon_F} \mathrm{Im}\ \ln(\Delta)\ d\epsilon - E_l - E_m - E_n \qquad (17)$$

Again, we shall use E_{lmn} as a shorthand to refer

to the three-adatom arrangement as well as their interaction energy. There are two aspects to this new interaction: (1) a new triangular path permitted electrons, represented by the G G G term, and (2) an "incompleted cubic" term, marked by the absence of V^8 and V^{12} terms that would be present in $E_l + E_m + E_n$ if their logarithms were merged. Trial calculations with moderate V appropriate to chemisorption sugggest that the "triangle path" gives a fair qualitative account of the full interaction.

Figure 5 displays the trio interaction energy plotted against ϵ_F of {100} cubium for previously used values of V and ϵ_a for four trio configurations that arise in a c(2 × 2) pattern on a square lattice surface. The trio energies apparently are dominated by the two closest (strongest) pairs. (Note that there is no E_1 [nearest neighbor] pair for this adlayer.) The two triads for which two of the "sides" are E_2 [second-nearest-neighbor] pairs have the strongest trio interaction energy; the one with E_3 as its third side, E_{223}, being somewhat more potent. With increasing adatom separation, the trio energies fall off rapidly, much like the pair energies.

Figure 6 answers the obvious next question of how these trio energies compare with pair energies. The E_{223} triad's trio energy is comparable to (although somewhat weaker than) the E_3 curve. Note that E_2 is plotted at *one third* its strength to make the graph clearer and to anticipate Section IVB; it is significantly stronger than the other two plotted energies.

B. Complete Overlayers

While quartets, quintets, *ad nauseum* could be generated, numerical noise problems would soon arise. Starting from the other end, we easily find that the interadatom *interaction* energy per adatom for a complete (1 × 1) adlayer is

$$-\frac{2}{\pi N_{\|}}\sum_{k_{\|}}\int_{-\infty}^{\epsilon_F}\mathrm{Im}\ln\{[(1-V^2\,G_{aa}(\epsilon)\,G(k_{\|},\epsilon)]/[1-V^2\,G_{aa}(\epsilon)\,G_{oo}(\epsilon)]\}\,d\epsilon$$

$$=-\frac{2}{\pi N_a}\sum_{k_{\|}}\int_{-\infty}^{\epsilon_F}\mathrm{Im}\ln[1-V^2\,\bar{G}_{aa}\{G(k_{\|},\epsilon)-G_{oo}(\epsilon)\}]\,d\epsilon \qquad (18)$$

where the summation goes over the surface Brillouin zone (SBZ), containing $N_{\|}$ (the number of surface sites) or, equivalently, N_a (the number of adatoms) points. The $G(k_{\|},\epsilon)$ are

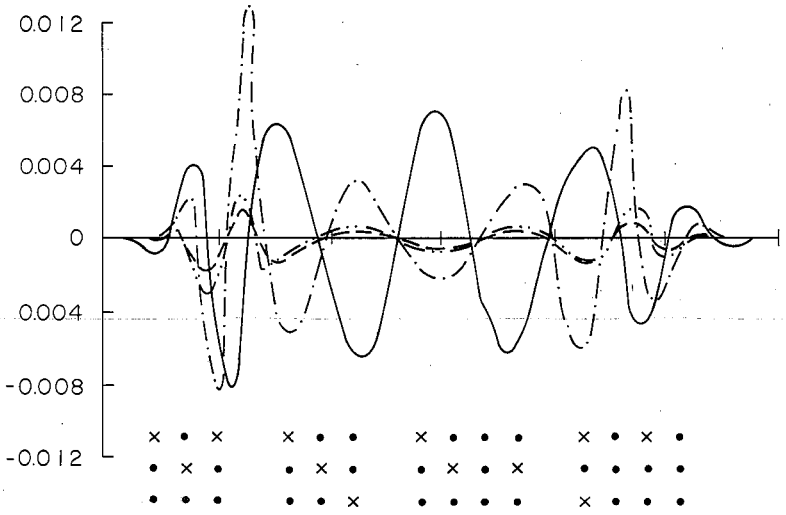

FIGURE 5. Trio interaction energy vs. substrate (cubium) Fermi energy for several configurations arising in a c(2 × 2) adlayer, as illustrated in the inset. The model parameters are atop binding, V = 3/2, and $\epsilon_a = -0.3$. From left to right in the inset, these trios (and the curves giving their interaction energies) are E_{223} (solid), E_{225} (dash-dot), E_{238} (dash-dot-dot), and E_{335} (dash).

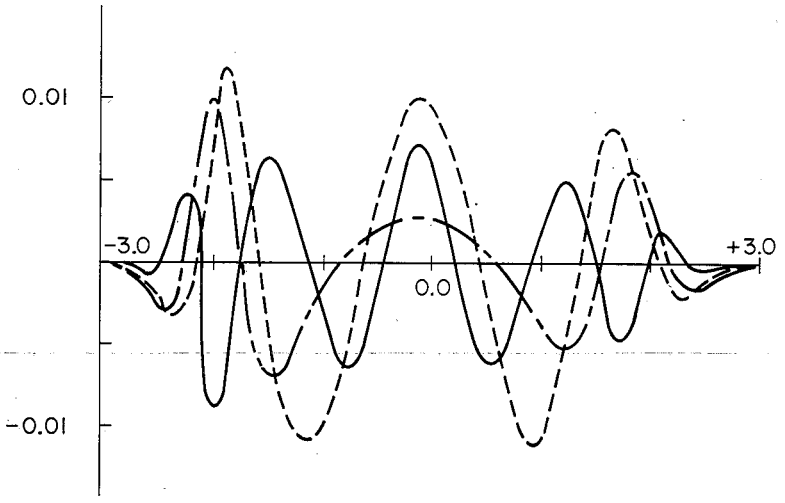

FIGURE 6. E_{223} trio interaction energy (solid curve), E_3 pair energy (dash-dotted curve), and *one-third* of the E_2 pair energy (dashed curve), all vs. Fermi energy, using the parameters of Figure 5. The curves are of comparable magnitude.

analytically computed[35] and were implicitly used above to form the G_{oj} according to

$$G_{ij}(\epsilon) = \frac{1}{N_{||}} \sum_{k_{||}} G(k_{||},\epsilon)\, e^{ik_{||}\cdot(R_i - R_j)} \qquad (19)$$

Thus, the lowest order (in $V^2\ \bar{G}_{aa}$) term in an expansion of the logarithm is of the order of $V^4\ \bar{G}_{aa}^2$, the coefficient being the sum of all possible G_{ij}^2 for i or j fixed, i.e., the lowest order contribution of the sum of all pairs.

As suggested by Burke's work,[23] neglect of any direct interaction for E_1 pairs on a square surface is a poor approximation, especially if the adatoms are comparable in size to the substrate atoms. Therefore, we focus on the c(2 × 2) overlayer. Since the real space unit cell area is doubled, the SBZ is halved, most naturally taking the form of an inscribed "diamond" (square rotated by 45° with dimensions decreased by $2^{-1/2}$). Points outside the new SBZ get folded back in, resulting in doubling of the [highly blurred] two-dimensional band structure. After much algebra, we find[71] that to describe a c(2 × 2) adlayer, we simply replace $G(k_{||},\epsilon)$ in the right-hand side of Equation 18 by

$$\{G(k_{||},\epsilon) - G(\pi(1,1) - k_{||},\epsilon)\}/2$$

Figure 7 shows the interadatom interaction energy (per adatom) for a full c(2 × 2) overlayer as a function of substrate filling. For comparison, we summed explicitly the pair energies for all pair configurations arising in a c(2 × 2) pattern (only the five shortest contribute significantly) weighting them according to the number per adatom existing in the pattern: two for pairs along the <10> and <11> mirror axes, four otherwise. This curve does a reasonable job of reproducing the c(2 × 2) plot, except perhaps near the half-filled substrate region, where the pair curve has the correct shape but only half the needed amplitude.[115] The trio curve gives an explicit sum of trio energies, again with the appropriate weighting factors. This curve helps make up the difference near the center of the band and is generally not too noticeable, except near energies corresponding to the Hartree-Fock bonding and antibonding resonances in the DOS. In short, trio energies are not too important in total overlayer energies, but may be significant for effects involving E_3 pairs,[72] such as discussed in Section IV.B.

C. Changes in Density of States

As suggested by Equations 7 to 9, the phase shift calculated to compute interaction energies can also be used to obtain the associated change in DOS. In Figure 8A, we display $\Delta\tilde{\varrho}$ (total DOS for adsorbed surface minus DOS for clean surface) for a single adatom in the atop position. The coupling V is moderately strong, approaching the regime in which the system can be viewed as an adatom-substrate neighbor sur-

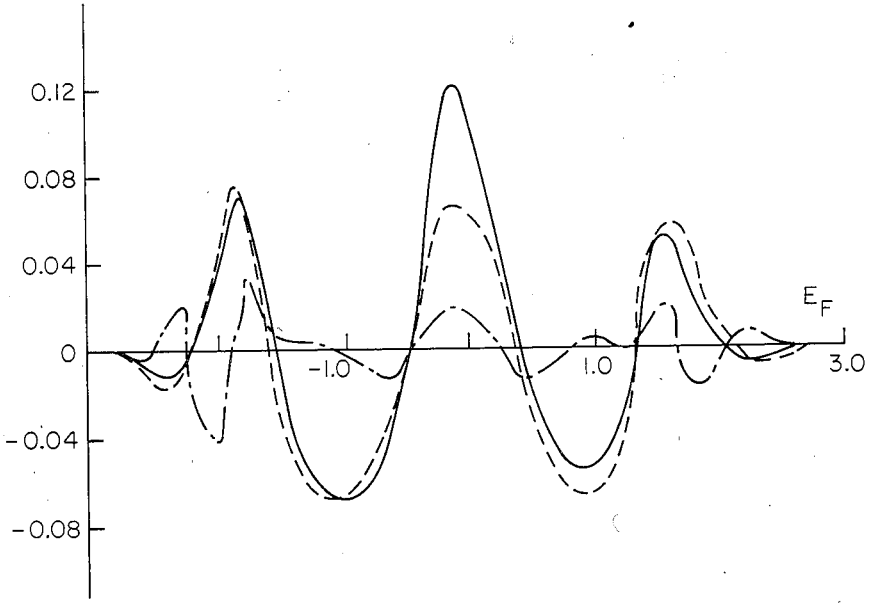

FIGURE 7. Lateral interaction energy per adatom (solid curve) vs. Fermi energy for a c(2 × 2) adlayer, with the parameters of Figure 5.[115] Also plotted are the sum of all pair interactions per adatom (dashed curve) in the layer and the trio interactions [actually just the dominant E_{223} and E_{225} contributions] per adatom (dash-dotted curve). Except near the band center, the pair curve closely follows the c(2 × 2) curve. (From Einstein, T. L., *Phys. Rev. B*, 16, 3411, 1977, in which the ordinate scale was 28% too large. With permission.)

face molecule rebonding to an indented solid. The spectrum accordingly is dominated by bonding and antibonding resonance peaks lying roughly equally on the adatom and its substrate neighbor.[16] Relative to the single-adatom curve, the E_2 pair contribution is strikingly large, especially in comparison with the very small ratio of the pair to single-adatom energy curves. Although there is some broad structure near the center of the band, the chief characteristic of the pair interaction is to split the bonding and antibonding resonances. Figure 8B repeats the E_2 pair interaction, along with the E_3 pair and the E_{223} trio as in Figure 6. The convergence is worse than for energies (the E_2 pair curve is not reduced by a third here). Figure 8A shows the outcome of summing to a full c(2 × 2) layer; we shall return to it after determining what significance to attach to these simple computations.

In the studies transcending Hartree-Fock[27-29] the local DOS on the adatom (the usually calculated quantity) is found to develop new peaks for physically reasonable intra-atomic repulsions U. For strong bonding, this new structure can be related to describing two-electron processes (e.g., shake-up) in a one-electron picture; for weak bonding, they correspond to atomic states. Again, we focus on the work of Schönhammer et al.,[12] as they are the only group to have considered two adatoms. Figure 9 depicts their results with and without correlation effects for the local DOS on one of two H atoms atop nearest-neighbor (E_1) sites of {100} cubium parameterized to resemble Ni. Their previous figure [not reproduced] shows the same two plots for just a single H. The only effect of the pair interaction is to broaden and split the bonding and antibonding peaks in each plot. The intensity and position of each of these peaks are unaltered. Moreover, the new correlation-induced peaks are apparently completely unaffected by the pair interaction. Since the shape of the splitting is similar in both plots, we suppose that Hartree-Fock calculations of pair or higher order changes in DOS should have at least qualitative utility.

Since the pair effects are sizeable, the change in DOS per adatom for a full adlayer would be expected to differ considerably from that for a single adatom. Ho et al.[13,14] studied chemisorption on the {100} face of a single-band tight-binding bcc crystal. The change in DOS for a

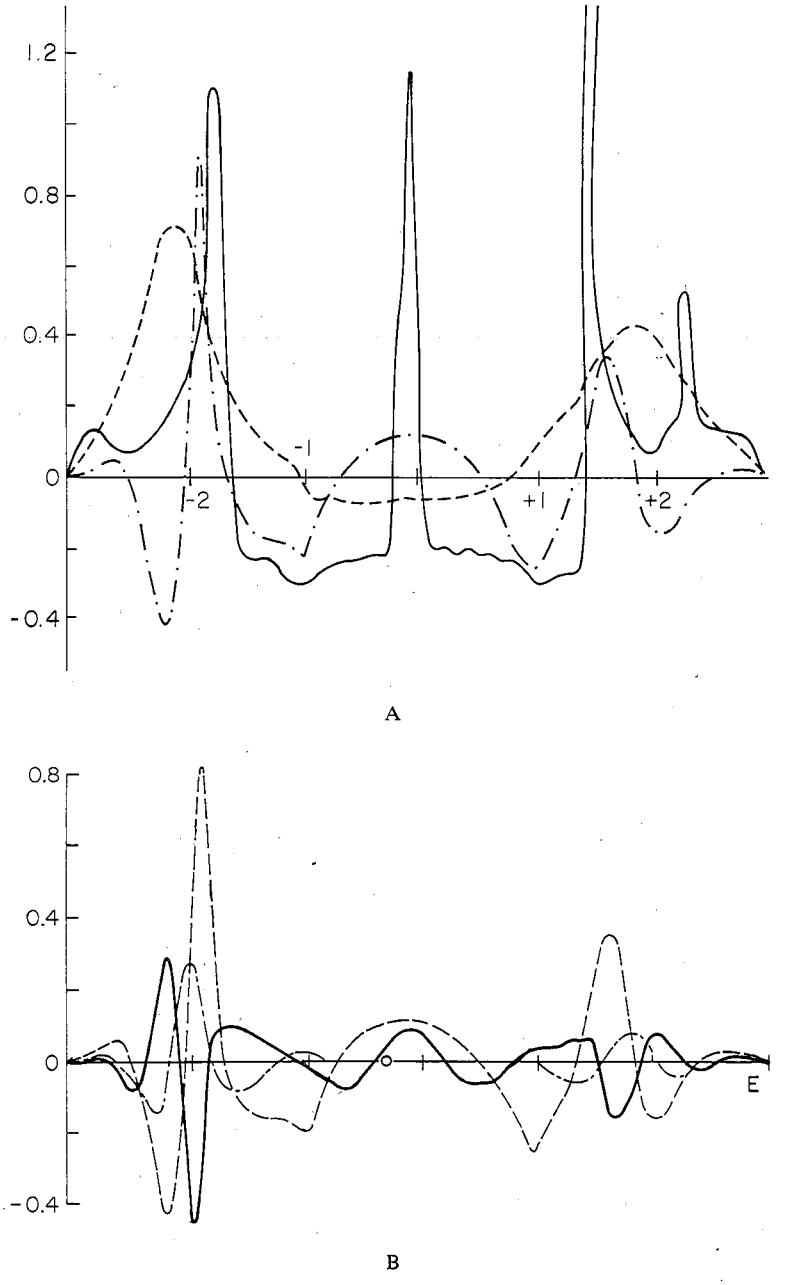

FIGURE 8. Contributions to total change in density of states per adatom, $\Delta\tilde{\varrho}(\varepsilon)$ vs. energy, with the parameters of Figure 5, germane to the c(2 × 2) overlayer: (A) single adatom (dashed curve), E_2 pair interaction (dash-dotted curve), and half $\Delta\tilde{\varrho}$ for a c(2 × 2) overlayer (solid curve). The c(2 × 2) curve includes [half] the single-adatom contribution. The peak at $E \sim 1.6$ extends to about 1.6. (B) ε_2 pair contribution again (dashed curve — same as dash-dotted curve in A), E_3 pair (dash-dotted curve), and E_{223} trio curve (heavy solid curve). (Adapted from Einstein, T. L., *Phys. Rev. B*, 12, 1262, 1975. With permission.)

single adatom in the centered position (i.e., the unoccupied lattice site) looks very similar to our result in Figure 8A; for the atop site, their curve is also rather like our result, except for a sharp dip at the center of the band brought on by the idiosyncratic band-center peak in the local DOS on the clean bcc surface. Figure 10 gives their result for a full (1 × 1) overlayer with atop bind-

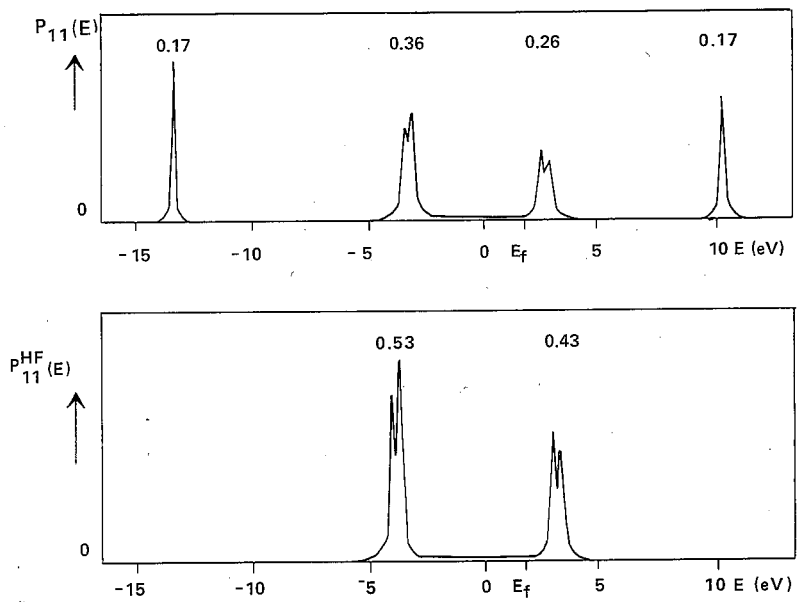

FIGURE 9. Local DOS on one of a pair of H atoms adsorbed on nearest-neighbor (E_1-type) sites, with the same parameters as in Figure 2. The upper curves are results of Schönhammer et al.;[12] the lower is Hartree-Fock. (From Schönhammer, K., Hartung, B., and Brenig, W., *Z. Phys. B*, 22, 143, 1975. With permission.)

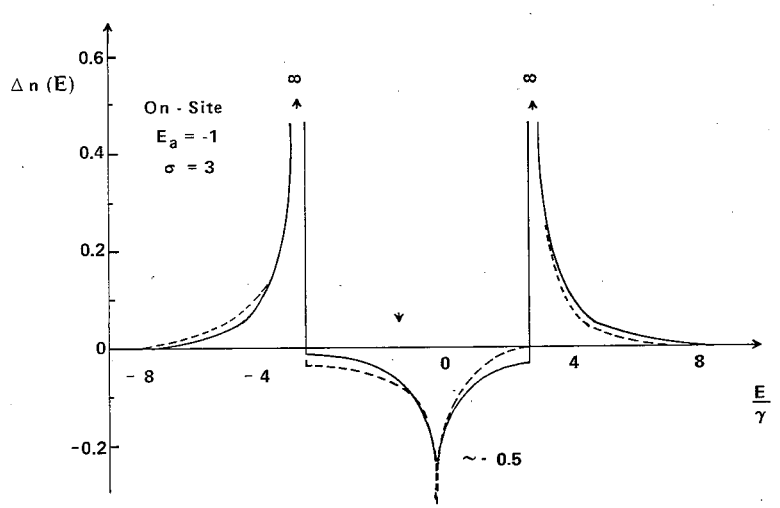

FIGURE 10. Total change in density of states per adatom ($\Delta n(\varepsilon)$ is our $\Delta\tilde{\varrho}$) for a monolayer of adatoms in the atop position on the {100} face of a semi-infinite single-band bcc crystal. The energy unit is (band width)/16; σ is our V. The solid curve is a non-self-consistent calculation for $\varepsilon_a = -1$; the dashed curve, for $E_a = 0$, is trivially self-consistent for a half-filled substrate band. (From Ho, W., Cunningham, S. L., and Weinberg, W. H., *Surf. Sci.*, 62, 662, 1977. With permission.)

ing. The bonding and antibonding peaks are narrowed and decidedly skewed. In the surface molecule limit, which they are nearing, the entire top layer of the crystal (i.e., the two-dimensional set of active orbitals) is peeled from the solid and each forms a molecule with an adatom. The dimer orbitals are modified by perturbative interactions among themselves and with the truncated substrate. This process involves moving what acts as the top layer of the crystal

one layer down, essentially removing one *bulk* layer; hence the negative region in the center of the band should reflect the *bulk* local DOS. Figure 10 also purports to indicate the effects of self-consistency, which in this case are rather minor; what is meant is imposing charge neutrality on the adatom by treating the adatom energy ε_a as a dependent variable (see Section II.C). Ho et al.[13,14] consider only the trivial case of a half-filled substrate, implying that ε_a be set at zero, the middle of the band. For centered binding, the results are more complicated.

Returning to Figure 8A, we seek the effect of a c(2 × 2) overlayer.[73] As in the (1 × 1) problem, the bonding and antibonding resonances are narrowed and strongly skewed. There is also some evidence of splitting, a good part of which is due to the E_2 pair contribution. [In the c(2 × 2) pattern, there are two E_2 pairs per adatom; since one half $\Delta\rho$ per adatom is plotted, direct comparisons are possible; the curve should be doubled in height to compare with the single-adatom curve.] In the strong binding limit, the top layer of substrate orbitals (now two per adatom) is again detached. The ones left undimerized in the c(2 × 2) pattern rebond weakly to the truncated substrate, giving a narrow peak near the substrate atomic energy (here at the center of the band). The behavior in Figure 8A verges on this regime.

As suggested in Section II.D, the object of DOS calculations is often to understand UV photoemission data.[74] Liebsch[75] has demonstrated the prominent role of final state effects — scattering of the photoelectron — in shaping the spectrum (particularly for angular-resolved experiments). It is thus disconcerting when DOS calculations for chemisorption are alleged to closely reproduce ultraviolet photoemission (UPS) difference spectra.[26] State-of-the-art calculations have now treated adsorbed monolayers of O on Ni{100}[76] and small clusters germane to chemisorption questions[77] as one-step processes in which initial and final states are generated in the same computer formalism, in the latter case including automatically (by virtue of the transition state) much of the relaxation effects. Again, the large computer-intensive nature of these techniques will limit their applicability to the pair problem for the present time.

IV. APPLICATIONS OF THE PAIR INTERACTION MODEL

A. Disordering Transitions for a Lattice Gas

Most problems in solid state involve several characteristic energies. When these energies are all of different magnitudes, analysis is greatly simplified. In lower coverage chemisorption on transition metals, such a hierarchy often exists. The strongest energy is the binding energy of an adatom, typically 2 to 7 eV.[15] Next comes the difference between binding energy in different substrate sites, which is of the order of the surface diffusion barrier and some moderate fraction of the binding energy.[78] Unlike physisorbed systems (e.g., Xe on Ag{111})[5,79] pair interaction energies here tend to be smaller than this second energy, causing adatoms to localize into particular positions relative to substrate atoms, between which they can hop at appropriate temperatures much less than desorption temperatures. The indirect pair interactions themselves form a hierarchy, generally falling off rapidly with pair separation.

In a specific application of this framework, Einstein and Schrieffer[15] pointed out how the pair interaction can explain the observed variety of adlayer superlattice structure. The first adatom in a neighborhood will select which binding site symmetry is the most favorable — atop, centered, or bridge on a square or hexagonal face, lattice, surface, bridge or atop on a {110} bcc, etc. All subsequent adatoms will occupy the same type of site. For a second adatom near the first, the most attractive of these sites is the one with the most attractive pair interaction, which is usually the first attractive interaction reached with increasing pair separation. A third nearby adatom will form a similar pair orientation with one of the first two, and so on to build up a pattern; that is, if the first attractive pair is the E_1, E_2, or E_3 pair, then the low-coverage adlayer pattern should be (1 × 1), c(2 × 2), or (2 × 2), respectively. This prescription is the source of the pattern assignments in Table 1.

To structure discussions more carefully, we use a lattice gas model, which is valid to the extent that (1) the discrete-site picture holds and (2) no neglected interactions creep in (e.g., dipole-dipole, magnetic, or trio). Since E_m is

the energy of the mth neighbor pair interaction (all implicit parameters — ε_F, V, etc. — being fixed).

$$H = \sum_m E_m \sum_{<ij>} n_i n_j \qquad (20)$$

where $<ij>_m$ denotes a sum over mth nearest neighbors without double counting. This model is equivalent to a [multineighbor] Ising model for localized spins[80]

$$H = -\sum_m J_m \sum_{<ij>_m} \sigma_i \sigma_j \quad -B \sum_j \sigma_j \qquad (21)$$

if one makes the identifications $n_j = (1 + \sigma_j)/2$, $E_m = -4J_m$ and adds

$$-(B - \Sigma_m J_m z_m)(2\theta - 1)N + (N/2)\,\Sigma_m J_m z_m \qquad (22)$$

to Equation 20. Here, θ is the fractional occupation and z_m is the number of mth nearest neighbors of a site (i.e., four or eight for a square lattice). The second term is an inconsequential constant, but the first is some effective magnitude field times $(2\theta - 1)$, the equivalent of total magnetization. In contrast to the Ising problem, $2\theta - 1$ is the variable over which one has experimental control, the conjugate field being the chemical potential. For theoretical calculations[81] it is often easier to treat the field as the independent variable adjusting it in the end to produce the proper θ, a common thermodynamic practice.

Since the Ising model is generally insoluble analytically, approximation schemes are required. In the preceding paper, Lagally referred to Monte Carlo methods used by Doyen et al.[82] for the case of just nearest-neighbor repulsion and calculations by Binder and Landau[81] for the case including second neighbors as well. We shall recapitulate these results before turning to some thoughts on the role of third neighbors.

Doyen et al.[82] simulate the approach to equilibrium of adatoms deposited randomly on a 30 × 30 square lattice. Figure 11A shows a half monolayer at a temperature a bit over half the order-disorder temperature for a full c(2 × 2) layer [viz., $E_1 = 1.76\ kT_c$]. After roughly 5 hops per adatom, the c(2 × 2) structure is clearly visible. Figure 11B repeats this calculation for $\theta = 0.35$ (and lower temperature). While there is merely one E_1 pair, the c(2 × 2) pattern is obscured (short-range order diminished) by the sparse coverage. After computing the lowering of the disordering temperature with decreasing coverage, Doyen et al. conclude that for less than $\theta = 0.3$, there is no clear ordering. This result is inconsistent with the many observed patterns at lower coverages;[83] the error lies, of course, in the neglect of any attractive interaction, which underpins the formation of islands. In particular, for c(2 × 2) islands an attractive E_2 is crucial.

The full c(2 × 2) overlayer has $\theta = 1/2$ and corresponds to an Ising antiferromagnet, with no external field. Describing the system now by a large positive E_1 and a weaker negative E_2, one finds an accurate approximate solution[84] for the order-disorder temperature:

$$e^{\beta_c E_1/2} = \sqrt{2}\, e^{-\beta_c |E_2|/2} + e^{-\beta_c |E_2|}, \quad \beta_c = (k_B T_c)^{-1} \qquad (23)$$

As expected, E_2 stabilizes the pattern; for $|E_2|/E_1 = 1/8$, the critical temperature rises to $E_1/1.5\ k_B$; for $|E_2|/E_1 = 1/2$, it is nearly E_1/k_B. Einstein and Schrieffer[15] inserted characteristic values of E_1 and E_2 into Equation 23 and found critical temperature of the same order of magnitude as Estrup's value[85] of 1/20 eV for H on W{100}. Estrup also noted the analogy between the intensity of adlayer-induced LEED spots and the Ising model [long-range] order parameter. Lagally and co-workers[86,87] have shown that this order-disorder transition is not the only kind that can arise. They worked on the analogous system of O on W{110}, which forms a (2 × 1) pattern describable in Ising terms by a rectangular lattice gas with two nearest-neighbor repulsions in $[1\bar{1}1]$ directions and two attractions for $[\bar{1}11]$ nearest neighbors and $[\bar{1}11]$ next-nearest neighbors. They found that an island dissolution phase transition can also produce the disordering; here, the island essentially evaporates into the [dilute] lattice gas. This behavior is derived from measurements of both adlayer-induced spot widths,[86] which show broadening characterizing loss of long-range order,[88] and spot intensities.[87] The dissolution transition gives information about the attractive pair energies alone since essentially no repulsive pairs are present. On the other hand, the order-disorder transition involves both attractive and repulsive pair energies. With data on both transitions, two pair energies can be obtained.[87]

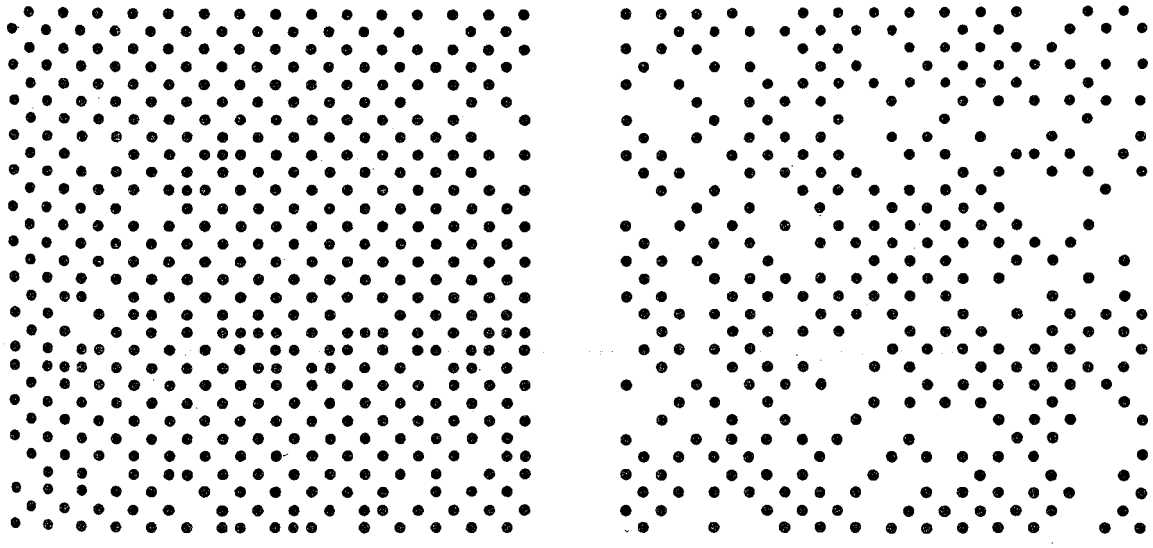

FIGURE 11. Results of a Monte Carlo simulation of ordering of adatoms on a square lattice. Particles are placed at random on a 30 × 30 lattice with only nearest-neighbor repulsion E_1. Configurations are after each particle has performed, on the average, five diffusion steps, (A) $E_1 = 3$ kT, $\theta = 0.5$; (B) $E_1 = 5$ kT, $\theta = 0.35$. (From Doyen, G., Ertl, G., and Plancher, M., *J. Chem. Phys.*, 62, 2957, 1975. With permission.)

On the theoretical side, Binder and Landau[81] have brought critical phenomena techniques to bear on adsorbed layers. With Monte Carlo methods, they construct T-θ phase diagrams for square lattice gases for E_1 positive and E_2/E_1 being $-1/2$, 0, and $+1/4$, with E_1 positive. For $E_2 < 0$, a complex diagram evolves; there are three different low-temperature ordered phases at various coverages: (2 × 2) near $\theta = 1/4$, c(2 × 2) with some mixing for intermediate θ, and (1 × 1) with (2 × 2) vacancies near $\theta = 3/4$. The diagrams all have a deceptive symmetry about $\theta = 1/2$, which in the Ising model corresponds to up-down spin symmetry. For $\theta > 1/2$, direct interactions will typically enter, as will new (weaker) binding states for adatoms,[89] which can be parameterized as three-adatom repulsions.

In spite of progress, many patterns still cannot be explained convincingly. For example, H on Mo{100} has a notoriously complicated phase diagram.[90] In particular, for $1/4 < \theta < 1/2$ instead of going directly from c(2 × 2) to disordered with increasing temperature, it goes through the intermediate "(4 × 2)" phase depicted in Figure 12. While the interaction energy per adatom is $2E_2 + 2E_3$ (to fourth neighbors) in the c(2 × 2) pattern, in the intermediate phase it is $1/2E_1 + E_2 + E_3 + 3E_4$. Since there is no ordered phase for $\theta < 1/4$, E_1 and E_2 (and presumably also E_3) are repulsive. There is no evidence mentioned of a (2 × 2) phase as in Binder and Landau's[81] theory. It is conceivable that if E_2 is comparable to $1/2\ E_1$ and E_4 is comparable to $1/3\ E_3$, this transition could be explained in terms of a minimal gain in entropy at the expense of a tiny change in pair energies. It would be surprising, however, if dipole-dipole forces, trio interactions, etc. did not enter into such a subtle competition. Behavior on {100} bcc surfaces should receive renewed interest in light of the reconstructive phase transitions found on clean Mo and W surfaces below room temperature;[91] this exotic behavior is most likely the source of the complexity.

B. Island Shapes

In the preceding section, it was shown that models including only a repulsive E_1 were incapable of describing low-coverage islands. Recent work[92] has shown that E_3 as well as E_2 is required to characterize c(2 × 2) islands on square lattice faces. From the outset, we presume that E_1 is large and, therefore, positive. E_2 must be negative [and, moreover, $E_2 < E_3$] so that c(2 × 2) [rather than (2 × 2)] will be the

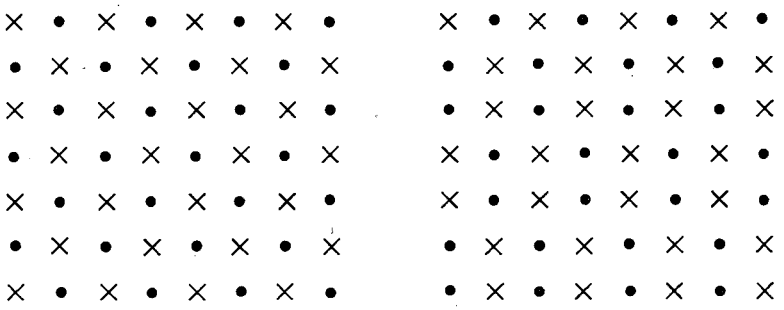

FIGURE 12. The two ordered phases that exist for H on the {100} face of Mo[90] at coverages between 1/4 and 1/2. Adsorbed sites are marked by crosses, vacant sites by dots (or vice versa; $\theta = 1/2$). The c(2 × 2) pattern at the left is stable below about 150 K; the so-called (4 × 2) at the right is stable above 190 K; between these temperatures is a mixed phase. (N.B., the [temperature at the] phase boundary rises considerably with increasing θ.)

low-coverage pattern. Finally, $E_3 < |E_2|$, since otherwise the stable arrangement would be simple lines in the direction of the E_2 bond (i.e., <11> relative to the substrate). If E_3 is negligible, the stable configuration of n^2 adatoms (n an integer) is a "diamond" (i.e., a square with sides along the <11> directions). On the other hand, if E_3 is comparable to E_2, the surface energy is roughly isotropic, favoring a more nearly circular domain, that is, a minimum perimeter configuration.

In the interior of a c(2 × 2) pattern, there are $2E_2$ and $2E_3$ pairs per adatom; at the edge, some are missing. By inspection, for an n × n [rotated] square (the "diamond"), there are $2n(n-1)$ E_2 bonds and $2(n-1)^2$ E_3 bonds. For example, if n is 11, there are $220E_2$ and $200E_3$ bonds, i.e., 22 missing E_2 bonds and 42 missing E_3 bonds. For circles, no simple formulas are possible; by an explicit (computer) count, there are 26 missing E_2 bonds and 34 missing E_3 bonds for a circle containing 121 adatoms. Even though the square has a longer perimeter, adatoms on a side are missing only one half rather than one E_2 bond each because of the <11> orientation. In this special case, the square has four fewer missing E_2 bonds and eight more missing E_3 bonds than the circle; hence, the square has the lower energy if E_3/E_2 is less than 1/2. For other special cases, one finds critical ratios down to 0.28. In the asymptotic limit we find[92] this ratio to be $(2-\sqrt{\pi})/2(\sqrt{\pi}-\sqrt{2}) \simeq 0.3176 \sim 1/3$. From Figure 6, we recall that this is roughly the ratio of the [envelopes of] E_3 and E_2; therefore, there should be examples of both in nature.

In fact, at absolute zero the stable shape of any large (i.e., describable as continuous) island will be a polygon, as predicted by Wulff's theorem.[93,94] If only attractive E_2 and E_3 are considered, this polygon is an equiangular octagon, i.e., the former square with truncated corners. The ratio of the length of the diagonal side (<10>) to that of the shortened square side (<11>) is $3E_3/\sqrt{2}\,(E_2 - E_3)$, which correctly vanished for $E_3 = 0$ and is unity for $E_3/E_2 \simeq 0.3204$, nearly the square-to-circle critical ratio. This octagonal form vanishes quickly at finite temperature.

When temperature effects are included for two-dimensional crystals, straight edges bow outward. Herring[95] notes that a straight side is in essence one-dimensional, long-range order and, hence, unviable above zero temperature. [Conjunctively, the Wulff plot cusps are removed by logarithmic entropy terms.] Also, the corners get rounded. In their classic study of crystal growth, Burton et al.[93] work out (in a quasicontinuous limit) the solution for domain shape as a function of temperature and the equivalent of E_2 and E_3 (although in their problem the lateral interactions were the same as the binding energies, so that disordering was related to desorbing). Defining β as $-E_2/kT$ and $\tilde{\beta}$ as $-(E_2 + 2E_3)/kT$, we can, after considerable algebra, reduce their expression to[92]

$$|y/u| = \tfrac{1}{2} + \tilde{\beta}^{-1}\left[\ln\{1 - (\sinh(\tilde{\beta}x/2u)/\sinh(\tilde{\beta}/4))^2\}\right.$$

$$\left. - \ln\left\{\frac{1 + f(\beta,\tilde{\beta})\cosh(\tilde{\beta}x/u)}{1 + f(\beta,\tilde{\beta})}\right\}\right] \qquad (24)$$

where $f(\beta,\tilde{\beta}) = (e^{\tilde{\beta}/2} - e^{\beta/2})/(e^{\beta/2}\cosh(\tilde{\beta}/2) - 1)$. Here, the x-y axes are <11> axes (i.e., the <10> axes of the c(2 × 2) adlayer) while u/2 is the maximum value of |x| and |y| and (0,0) is the center of the figure. This expression only holds for $|y'(x)/u|$ less than unity, but by taking advantage of fourfold symmetry, one can reflect the curve through the lines $y = \pm x$ to obtain the right and left quadrants. Matching problems are insignificant for the parameters of interest.[92]

If $E_3 = 0$, $\tilde{\beta} = \beta$, and so $f(\beta,\tilde{\beta})$ vanishes, as does the second logarithm in Equation 24. In Figure 13, equilibrium island shapes are plotted for $\beta = 4$, 6, 8, and 10. As $T \to 0$, the curves approach a square. For smaller β, remnants of the square shape wash out, so that by $\beta = 4$ the plot is scarcely distinguishable from a circle. For still smaller β, the analysis breaks down.[92,93]

From Figure 6, one can estimate $-E_2$ to be of the order of 0.01 to 0.03 times one sixth the bandwidth, i.e., roughly 10 to 60 meV or 120 to 700 K in temperature units for transition metals. [For comparison, from Burke's work,[23] we find that the curve of second-neighbor pair energy for a {100} bcc surface looks rather similar to that on the {110} surface exhibited in Figure 3A; E_2 is repulsive near the center of the band, so W/W(100) is not c(2 × 2). When E_2 is attractive, its magnitude is of the order of 100 meV.] The smallest β for which one could see square-like structure seems to be about 8, indicating temperatures in the range 15 to 88 K. Alternatively, from Equation 23, if $E_1/|E_2|$ is 2, 4, 6, or 8, then $-\beta_c E_2$ is 0.521, 0.327, 0.238, or 0.187, respectively. Thus, a β of 8 corresponds to 1/15 to 1/43 T_c or about 15 to 40 K.

For E_3 finite, Equation 24 suggests that the temperature enters almost entirely through $\tilde{\beta}$. Since $\tilde{\beta}$ is the dimensionless constant formed by (twice) the ratio of the energy per unit length

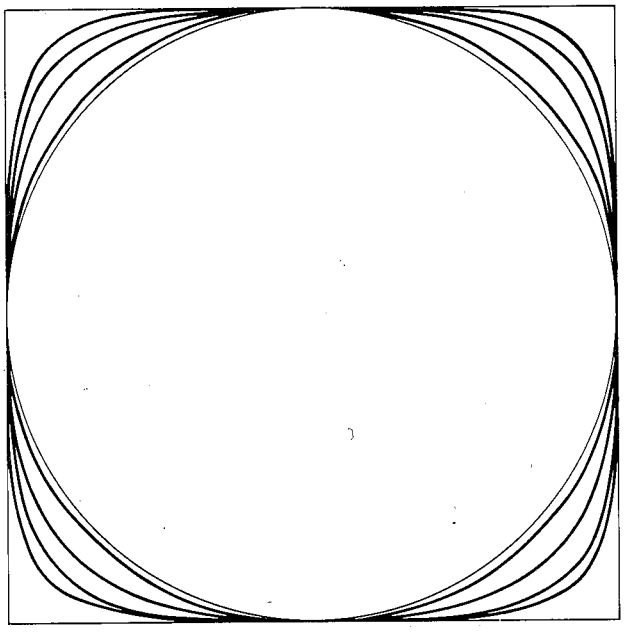

FIGURE 13. Shape of c(2 × 2) islands as a function of temperature, for the special case $E_3 = 0$, using Equation 24. The picture assumes no nearest-neighbor occupation ($E_1 >> |E_2|$) and a moderately large island. At zero temperature, the stable island shape is square, with sides along the substrate <11> directions (i.e., the <10> axes of the adlayer when viewed as a square). As temperature rises, the sides bow out (if there were normalized area) and the corners round off. The plots are $kT/(-E_2) = 1/10$, 1/8, 1/6, and 1/4. The analysis collapses when (or before) the plot resembles a circle (i.e., a ratio of 1/3 to 1/2).

of a square side (x or y edge) to T, the primary role of temperature is to destabilize these edges. To obtain finite T shape-change behavior as a function of E_3/E_2 corresponding to the zero T results, one should hold $\tilde{\beta}$ rather than β constant, as explicit plots verify.[92] This feature is not promising for actual experiments, since E_3/E_2 is a fixed property of the system. LEED is the experimental method most suitable for investigating island shapes. Consider first an n × n [rotated] square of adatoms. The problem is reminiscent of Fraunhofer diffraction through a square aperature, leading to (1) bright central maximum of size $2\pi/nd$ by $2\pi/nd$ in K space, K being the scattering vector and d the c(2 × 2) adatom lattice constant, $\sqrt{2}$ times that of the substrate and (2) subsidiary maxima in the <11> (with respect to the substrate) directions in K space. In real situations, there will be a distribution of sizes, washing out the nodes between the subsidiary maxima, leaving a four-lobed star.[96] These stars should be present just at LEED spots due only to the adlayer, i.e., (1/2, 1/2) spots in this case.

Numerous complications modify this simple picture. The finite-temperature bowing of square sides will flare out the lobes of the star.[97] The rounded corners will scatter into the region outside the lobes. Explicit computer simulations[96] give detailed information as to how these features affect intensity. Islands will, in general, not have their equilibrium shape. Herring[98] notes that the relevant questions concern the local equilibrium shape: how to minimize [free] energy with a minimum of atom relocation. Thus, rather than square-like islands, one may often see a strong tendency to rectangular steps at island edges.

For this work, the island size should be smaller than the LEED coherence zone, which has a typical diameter of 100 Å,[82,86,99] but can be modified over a moderate range by adjusting beam energy and angles.[99] Lu et al.[87] report a mean diameter of 35 Å for 0 (2 × 1) islands on W(110), which is smaller than optimal for our procedure. Since the islands should be well separated, this work is complementary to Park and Houston's use of domain mismatch to study binding sites.[100] One must also consider the fact that these islands are often not in equilibrium, so that even detailed work in the spirit of Binder and Landau[81] may not answer all questions. By correctly cycling temperature, it should be possible to engineer a variety of configurations. Work is in progress to study these matters.[92,96]

V. CONCLUSIONS AND PROSPECTS

The indirect electronic pair interaction has been confirmed as the principal mode of interaction between many kinds of atoms chemisorbed on transition metal substrates. The dipole-dipole interaction may also be important under some circumstances. Other [indirect] interactions should not be important for most energy features.[116]

Coulombic effects turn out in model systems to be much less important in pair problems than in single-adatom problems. This suggests that in order to narrow the gap between theoretical and experimental numbers, effort may be better spent on implementing improved substrate intermediate states than on working on correlation effects with simplified substrates. Progress will come first on third-row late-transition and noble element substrates, where s-p hybridization and spin-orbit coupling are not so important. Various non-self-consistent tight-binding calculations for Ni, Cu, and Fe have appeared.[52,53,57] While their DOS might not be as accurate as desired, it would be of interest to determine what details about pair interactions one might generate. Such calculations would also be useful in determining the potency of trio interactions.[117] Recent work[101,102] has also found that the s-electrons in Ni may play a major role in chemisorption. More difficult [noncluster] calculations will probably be needed to determine if the same result holds for pair interactions.

Unfortunately, these materials are not well suited for field ion microscopes. It is a long calculational road through the periodic table to get from Ni to W and Re. Prospects for significant improvement beyond Burke's work seems rather remote. Thus, any theoretical work on the new experiments for W on W with dilute Re impurities,[103] for example, will at best be at a semiquantitative level.

Imbedded cluster calculations may have some impact on the pair problems either using one large cluster or two small ones. Clusters may well be more important in sorting out the

role of direct interactions, which are crucial to dissociation processes on surfaces and, hence, to most industrial applications.

Phase transitions is another fruitful area. We have seen the progress that has been made experimentally. Accompanying model calculations to simulate and test experimental situations are now quite relevant. In order to make progress for higher coverage ($\theta > 1/2$) substrates, more input about direct interactions, trio interactions,[117] and adsorption strengths in nonsymmetric positions will be needed. There is a rich variety of phenomena[89,104] in this regime awaiting theoretical analysis.

If findings concerning pair interactions and more general problems of chemisorption can be applied to materials science, an enormous increase in understanding questions such as hardness and embrittlement will result. Latanision[105] reviews the considerable modifications that chemisorption can bring about in the strength of solids. Much of the role arises from the fact that dislocations and cracks start most readily on surfaces. Relevant questions include:

1. How does local lattice strain relate to chemisorption bond strength?[106] An analogous pair question is whether there exist strain-induced adlayer superlattice phase transformations.
2. Conversely, how does a chemisorption bond affect nearby substrate bonds? While ionically adsorbed species may simply transfer electrons to or from the substrate, shifting the band filling (in "rigid band" fashion), covalently adsorbed atoms tend to form "surface molecules", thereby weakening substrate bonds between the [bulk] chemisorbing atoms and their neighbors. The details of this effect can be readily pursued in model systems.[71]
3. How do adatoms interact with substrate impurities? Recent work by Tsong and Cowan[103] is in this direction.
4. What factors influence whether an atom adsorbs onto or absorbs into a metal? In this regard, studies of surface segregation, as reviewed by Blakely,[107] prove helpful.
5. In particular, to what degree are hydrogen's unique electronic structure and size responsible for its potency in embrittling metals? How does its diffusion through a metal compare with that on a surface, and how are both modified by the presence of defects in the form of impurity [ad]atoms, dislocations, etc.? The problems are manifold and inviting.

It is unfortunate that symmetry conditions prevent the use of the many excellent slab computation schemes for studying pair interactions. The best that can now be hoped for is consideration of c(2 × 2) overlayers. Perhaps a periodic net of large unit cells with various pair orientations can eventually be implemented.

Overall, then, basic understanding of the problem is fairly good, but many details need to be clarified. Order-of-magnitude numerical fits to data are typically possible, but 10% matching is not.

VI. ACKNOWLEDGMENTS

This work was supported in part by the National Science Foundation under Grant DM-76-82519. The University of Maryland Computer Science Center supplied computer time and use of their facilities. I am also grateful for valuable comments and suggestions from Professors M. G. Lagally (for alerting me to References 81 and 108) and M. B. Webb and for innumerable helpful discussions with the various members of the University of Maryland Solid State Theory and Surface Physics groups.

VII. APPENDED NOTE: ASYMPTOTIC RESULTS

After the writing of the preceding manuscript, a preprint by K. H. Lau and W. Kohn entitled "Oscillatory Indirect Interaction Between Adsorbed Atoms" was received.[108] Briefly, they corroborate the $\cos(2k_F R)/R^5$ asymptotic behavior of the pair interaction and point out the possibility of a $\cos(2k_F R)/R^2$ interaction due to partially filled band of surface states, carefully showing how these dependencies arise from singularities related to the Fermi surface. Since these asymptotic results are so pertinent to this review, this section has been added.

Preliminarily, they expand the [exact] static density response function[109] for a sine-wave gas

(i.e., electrons confined to half of space by an infinite potential barrier). For two points near the edge, it goes as $\cos(2k_F R)/R^5$ to lowest order in R, the lateral separation.

Lau and Kohn proceed to verify that two bare charges near a [noninteracting] electron gas confined by a finite barrier (i.e., a jellium background) interact similarly. Treating the adatom-substrate interaction potential in second-order perturbation theory, they can separate the pair energy from the single-adatom energy, reminiscent of but different from Equation 12. The R dependence of the pair interaction reduces to

$$\int d^2q\, e^{i\underline{q}\cdot\underline{R}}\, G(\underline{q}) \tag{25}$$

where q is momentum transfer parallel to the surface and G(q) is a kernel which depends only on the substrate energy spectrum (here free electron) and the justified assumption that small k_z dominates, not on the form of the one-electron potential near the surface nor the form of the adatom-substrate coupling. Detailed analysis shows that the asymptotic dependence is dominated by a singularity in the fourth derivative of G(q) at $2k_F$, times a step (Heaviside) function; with the aid of Lighthill's formulas[109] for generalized functions, Equation 25 reduces to

$$-\pi^3\, k_F{}^3 \cos(2k_F R)/R^5 + \theta\left[\frac{1}{R^6}\right] \tag{25a}$$

The asymptotic pair energy is the product of Equation 25a and expressions involving the interaction of the individual adatoms with the substrate. The result is consistent with Grimley's[8,31] since one can view any direction on a jellium surface as critical. However, the estimated magnitude for (H/Al parameters) is less than 1 meV at the relevant separations.

In an analogous calculation, Lau and Kohn consider the form of an indirect interaction mediated by a partially filled parabolic surface band (with a consequent cylindrical Fermi surface). The singular nature of G(q) at $2k'_F$ (where k'_F is the Fermi wave vector for the surface band) now appears in its first derivative, leading to $\cos(2k'_F R)/R^2$ behavior. To gauge the prefactor, Lau and Kohn couple bare charges electrostatically to model surface wave functions and parametrize the results with bulk Al values. We find that the resulting energy estimate (in electron volts) is $-3.7\cos(2k'_F R)/(2k'_F R)^2$, where $2k'_F R$ is 10.38 times the separation in units of the Al nearest-neighbor distance; hence, $E_2 = +8.9$ meV and $E_3 = +2.9$ meV. Even more dramatic is the possibility of a $\cos(k_o R)/R$ effect in directions normal to parallel planes on the Fermi surface that are k_o apart. Although Tsong earlier reported such behavior,[60] uncertainties have arisen as to how the interaction decays with R.[103] Future developments will be quite interesting.

Near the band edge of the single band, simple-cubic crystal [in the tight-binding model] cited extensively in the text, the band structure reduces to the simple parabolic form. Accordingly, Lau and Kohn seek similar $\cos(2k_F R)/R^5$ behavior for the pair interaction in this model. Since straightforward perturbation theory would obviously (Equations 11 to 14) require computing the fourth-order contribution of $\mathcal{H}' \equiv \mathcal{H}_{am} + \mathcal{H}_{bm}$, they use a canonical transformation to eliminate $\mathcal{H}'$ to lowest order. In essence, this procedure is a generalization of the Schrieffer-Wolff transformation.[111] A second-order perturbation calculation produces an expression to which the preceding jellium techniques are applied, with the result

$$E_n = \frac{V^4}{(\epsilon_F - \epsilon_a)^2}\left[\frac{k_F}{\pi}\right]^3 \frac{\cos(2k_F R_n)}{R_n{}^5} \tag{26}$$

where the unit of length is the lattice constant, R_n is the nth neighbor separation, and k_F is $\sqrt{2(3 + \epsilon_F)}$ (since we measure energies from the center of the band rather than the bottom). Intrinsic to this asymptotic regime is the expansion of Equation 13 to obtain Equation 14, i.e., that $V^4 G_{on}{}^2 \bar{G}_{aa}{}^2$ be small. Note that this smallness can always be achieved through G_{on} for moderate R_n, with no weak-V assumption. If V is taken as small, no characteristic surface molecule is formed; the adatom level is merely broadened and shifted. Consistent with this picture is the neglect of the renormalization of the adatom due to its bonding to the surface, [as manifested formally by the presence of $\bar{G}_{aa}$ rather than G_{aa} in Equations 13 and 14. The $(\epsilon_F - \epsilon_a)^{-2}$ in Equation 26 is just $G_{aa}{}^2(\epsilon_F)$.] Lau and

Kohn observe a related resonance in their formalism for $\varepsilon_F \approx \varepsilon_a$; alas, this regime is the most interesting since [covalent] adsorption is strongest and charge transfer/self-consistency problems are least.

Even when Equation 14 is valid, the substrate propagator G_{on} is far from its asymptotic form at near-neighbor separations. Equation 26 implicitly assumes that (using advanced Green's functions)[15,35]

$$G_{on}(\epsilon) = -\frac{ik}{\pi R_n^2} e^{-ikR_n} \tag{27}$$

where again k is $\sqrt{2(3+\varepsilon)}$. Using the exact form of $G(k_\parallel,\varepsilon)$, Lighthill's formulas,[110] and stationary phase integrations, we have calculated[19,112] the asymptotic behavior of G_{on} in the two mirror directions for any energy: in the upper or lower third of the band ($|\epsilon| > 1$)

$$G_{on}(\epsilon) = \begin{cases} -\frac{i}{\pi R_n^2}\sqrt{(3-|\epsilon|)\ (|\epsilon|-1)}\ \exp\left[-iR_n \cos^{-1}\{(2-|\epsilon|)\mathrm{sgn}(\epsilon)\}\right], \hat{R}_n = \langle 10\rangle \\ -\frac{i}{\pi R_n^2}\sqrt{\frac{(3-|\epsilon|)(1+|\epsilon|)}{(|\epsilon|-1)}}\ \exp\left[-i\sqrt{2}\,R_n \cos^{-1}\{\tfrac{1}{2}(1-|\epsilon|)\,\mathrm{sgn}(\epsilon)\}\right], \hat{R}_n = \langle 11\rangle \end{cases} \tag{28}$$

which [both] reduce to Equation 27 for $\varepsilon \gtrsim -3$. (Here, $\mathrm{sgn}(\varepsilon) \equiv \varepsilon/|\varepsilon|$.) In the central third of the band, the appropriate continuations of the Green's functions in the outer thirds add together. In the <10> (but not the <11>) case, this leads to the vanishing of G_{on} to order $1/R_n^2$.[118] Taking advantage of the oscillatory nature of Equation 28, we can integrate Equation 14 by parts to get

$$E_n \sim \frac{V^4}{R_n} \mathrm{Re}\{\overline{G}_{aa}^{\,2}(\epsilon_F)\, G_{on}^{\,2}(\epsilon_F)\} \tag{29}$$

which decays like R_n^{-5} at least in the mirror directions; in the central third of the band, the <10> fall-of is even faster.

Detailed comparisons[19,112] of Equations 13 and 29, i.e., the exact values of Re G_{on}^2 with those given by Equation 28, show that the asymptotic limit is achieved only for R_n so large (several lattice spacings) that E_n is negligible, in sharp contrast to the interaction of localized magnetic moments in a bulk electron gas.[113] Even near the band edge, where the density of states is small, the asymptotic form is not generally useful at small R_n, essentially since the asymptotic assumption $k_F R_n >> 1$ breaks down. In this regime, the adatoms couple to the lowest bonding Bloch states of the substrate; since their wavelengths are long compared to R_n, the adatoms couple in phase. Hence, the pair interaction is uniformly attractive. Correspondingly, near the top of the band, the substrate orbitals are maximally out of phase. The sign of the interaction alternates with each lattice step of separation.

REFERENCES

1. Grimley, T. B., *CRC Crit. Rev. Solid State Sci.*, 6(3), 239, 1976.
2. Appelbaum, J. A. and Hamann, D. R., *Rev. Mod. Phys.*, 48, 479, 1976; *CRC Crit. Rev. Solid State Sci.*, 6(4), 359, 1976.
3. Davenport, J. W., Einstein, T. L., Schrieffer, J. R., and Soven, P., *The Physical Basis for Heterogeneous Catalysis*, Drauglis, E. and Jaffee, R. I., Eds., Plenum Press, New York, 1975, 295.

4a. Melius, C. F., Moskowitz, J. W., Mortola, A. P., Baillie, M. B., and Ratner, M. A., *Surf. Sci.*, 59, 279, 1976.

4b. Schrieffer, J. R., *J. Vac. Sci. Technol.*, 13, 335, 1976.

5. Kohn, W. and Lau, K. H., *Solid State Commun.*, 18, 553, 1976; see also Lannoo, M. and Allan, G., to be published.

6a. Hirschfelder, J. O., Curtiss, C. F., and Bird, R. B., *Molecular Theory of Gases and Liquids*, John Wiley & Sons, New York, 1954.

6b. Margenau, H. *J. Chem. Phys.*, 9, 896, 1938.
6c. Barker, J. A., Watts, R. O., Lee, J. K., Schafer, T. P., and Lee, Y. T., *J. Chem. Phys.*, 61, 3081, 1974.
6d. Axilrod, B. M. and Teller, E., *J. Chem. Phys.*, 11, 299, 1943; Muto, Y., *Proc. Phys. Math. Soc. Jpn.*, 17, 629, 1943.
6e. Sinanoglu, O. and Pitzer, K. S., *J. Chem. Phys.*, 32, 1279, 1960.
6f. McLachlan, A. D., *Mol. Phys.*, 7, 381, 1964.
6g. MacRury, T. B. and Linder, B., *J. Chem. Phys.*, 54, 2056, 1971.
6h. Freeman, D. L., *J. Chem. Phys.*, 62, 4300, 1975.
6i. Bruch, L. W., Cohen, P. I., and Webb, M. B., *Surf. Sci.*, 59, 1, 1976.
6j. Rehr, J. J., Zaremba, E., and Kohn, W., *Phys. Rev. B*, 12, 2062, 1975.
7. Hoffmann, R., *Acc. Chem. Res.*, 4, 1, 1971.
8a. Grimley, T. B., *Proc. Phys. Soc.* (London), 90, 751, 1967.
8b. Grimley, T. B., *Proc. Phys. Soc.* (London), 92, 776, 1967.
8c. Grimley, T. B., *J. Am. Chem. Soc.*, 90, 3016, 1968.
9. Anderson, P. W., *Phys. Rev.*, 124, 41, 1961.
10. Alexander, S. and Anderson, P. W., *Phys. Rev. A*, 133, 1594, 1964.
11. Hubbard, J., *Proc. R. Soc. London Ser. A*, 276, 238, 1963.
12. Schönhammer, K., Hartung, V., and Brenig, W., *Z. Phys. B*, 22, 143, 1975.
13. Ho, W., Cunningham, S. L., and Weinberg, W. H., *Surf. Sci.*, 54, 139, 1976.
14. Ho, W., Cunningham, S. L., and Weinberg, W. H., *Surf. Sci.*, 62, 662, 1977.
15. Einstein, T. L. and Schrieffer, J. R., *Phys. Rev. B*, 7, 3629, 1973.
16a. Einstein, T. L., *Phys. Rev. B*, 12, 1262, 1975.
16b. Einstein, T. L., *Surf. Sci.*, 45, 713, 1974.
17. Grimley, T. B., *J. Phys. C*, 3, 1934, 1970.
18. Grimley, T. B., in *Dynamic Aspects of Surface Physics*, Goodman, F. O., Ed., Editrice Composition, Bologna, 1974.
19. Einstein, T. L., Ph.D. thesis, University of Pennsylvania, Philadelphia, 1973.
20. Bagchi, A. and Cohen, M. H., *Phys. Rev. B*, 9, 4103, 1974; Lyo, S. K. and Gomer, R., *Phys. Rev. B*, 10, 4161, 1974.
21. Löwdin, P. O., *J. Chem. Phys.*, 18, 365, 1950.
22. Birkhoff, G. and MacLane, S., *A Brief Survey of Modern Algebra*, 2nd ed., Macmillan, New York, 1965.
23. Burke, N. R., *Surf. Sci.*, 58, 349, 1976.
24. Schrieffer, J. R., *J. Vac. Sci. Technol.*, 9, 561, 1972.
25. Mulliken, R. S., *J. Phys.*, 2, 782, 1934; Santry, D. P. and Segal, G. A., *J. Chem. Phys.*, 47, 158, 1966; Pople, J. A. and Beveridge, D. L., *Approximate Molecular Orbital Theory*, McGraw-Hill, New York, 1970, 77.
26. Pandey, K. C., *Phys. Rev. B*, 14, 1557, 1976.
27. Brenig, W. and Schönhammer, K., *Z. Phys.*, 267, 201, 1974.
28. Hertz, J. A. and Handler, J., *Phys. Rev. B*, 15, 4667, 1977.
29. Bell, B. and Madhukar, A., *J. Vac. Sci. Technol.*, 13, 345, 1976; *Phys. Rev. B*, 14, 4281, 1976.
30. Newns, D. M., *Phys. Rev.*, 178, 1123, 1969.
31. Grimley, T. B. and Walker, S. M., *Surf. Sci.*, 14, 395, 1969.
32. Grimley, T. B., in *Structure and Properties of Metal Surfaces*, Vol. 1, Shimodaira, S., Ed., Aruzen, Tokyo, 1973, 72.
33. Kim, D. J. and Nagaoka, Y., *Prog. Theor. Phys.* (Kyoto), 30, 743, 1963.
34. Ruderman, M. A. and Kittel, C., *Phys. Rev.*, 96, 99, 1954; Yosida, K., *Phys. Rev.*, 106, 893, 1957; VanVleck, J. H., *Rev. Mod. Phys.*, 34, 681, 1962.
35. Kalkstein, D. and Soven, P., *Surf. Sci.*, 26, 85, 1971.
36. Friedel, J., *Philos. Mag. Suppl.*, 3, 466, 1954; *Nuovo Cimento Suppl.*, 7, 287, 1958.
37. Allan, G., *Ann. Phys.* (Paris), 5, 169, 1970; Bruneel, C. and Allan, G., *Surf. Sci.*, 39, 385, 1973.
38. Leynaud, M. and Allan, G., *Surf. Sci.*, 53, 359, 1975.
39. Rudnick, J. and Stern, E. A., *Phys. Rev. B*, 7, 5062, 1973.
40. Allan, G. and Lenglart, P., *Surf. Sci.*, 30, 641, 1972.
41. Grimley, T. B. and Torrini, M., *J. Phys. C*, 6, 868, 1973; Grimley, T. B., *Ber. Bunsenges. Phys. Chem.*, 75, 1003, 1971.
42. Hyman, E. A., *Phys. Rev. B*, 11, 3739, 1975.
43. Grimley, T. B. and Pisani, C., *J. Phys. C*, 7, 2831, 1974.
44. Kjöllerström, B., Scalapino, D. J., and Schrieffer, J. R., *Phys. Rev.*, 148, 665, 1966.
45. Zubarev, D. N., *Sov. Phys. Usp.*, 3, 320, 1960.
46. Einstein, T. L., *Phys. Rev. B*, 11, 577, 1975.
47. Schönhammer, K., *Z. Phys. B*, 21, 389, 1975; see also *Phys. Rev. B*, 13, 4336, 1976.
48. Lang, N. D., *Solid State Phys.*, 28, 225, 1973; Smith, J. R., Ying, S. C., and Kohn, W., *Phys. Rev. Lett.*, 30, 610, 1973; Lang, N. D. and Williams, A. R., *Phys. Rev. Lett.*, 34, 531, 1975; Gunnarsson, O. and Hjelmberg, H., *Phys. Script.*, 11, 97, 1975.
49. Appelbaum, J. A. and Hamann, D. R., *Phys. Rev. B*, 6, 2166, 1972; *Phys. Rev. Lett.*, 32, 225, 1974.
50. Alldredge, G. P. and Kleinman, L., *Phys. Rev. B*, 10, 559, 1974; Schlüter, M., Chelikowsky, J. R., Louie, S. G., and Cohen, M. L., *Phys. Rev. B*, 12, 4200, 1975.

51. Tosatti, E., in *Proc. 13th Int. Conf. Semiconductors,* Fumi, F. G., Ed., Marves-North-Holland, Rome, 1976, 21.
52. Terakura, K., *J. Phys. Soc. Jpn.*, 34, 1420, 1973.
53. Davenport, J. W., Einstein, T. L., and Schrieffer, J. R., *Jpn. J. Appl. Phys. Suppl.*, 2, 691, 1974.
54. Kasowski, R. V., *Phys. Rev. Lett.*, 33, 1147, 1974; Batra, I. P. and Ciraci, S., *Phys. Rev. Lett.*, 39, 774, 1977.
55. Cooper, B. R., *Phys. Rev. Lett.*, 30, 1316, 1973; Kar, N. and Soven, P., *Phys. Rev. B,* 11, 3761, 1975; Kohn, W., *Phys. Rev. B,* 11, 3756, 1975.
56. Kasowski, R. V., *Phys. Rev. Lett.*, 33, 83, 1974.
57. Dempsey, D. G., Kleinman, L., and Caruthers, E., *Phys. Rev. B,* 12, 2932, 1975; 13, 1489, 1976; 14, 279, 1976; Sohn, K. S., Dempsey, D. G., Kleinman, L., and Caruthers, E., *Phys. Rev. B,* 13, 1515, 1976; 14, 3185, 1976; 14, 3193, 1976.
58. Gay, J. G., Smith, J. R., and Arlinghaus, F. J., *Phys. Rev. Lett.*, 38, 561, 1977; Proc. 37th Annu. Conf. Physical Electronics, Stanford, June 20 to 22, 1977.
59. Appelbaum, J. and Hamann, D. R., Proc. 37th Annu. Conf. on Physical Electronics, Stanford, June 20 to 22, 1977.
60. Tsong, T. T., *Phys. Rev. B,* 6, 417, 1972; 7, 4018, 1973; *Phys. Rev. Lett.*, 31, 1207, 1973.
61. Tsong, T. T., Cowan, P., and Kellogg, G., *Thin Solid Films,* 25, 97, 1975.
62. Bassett, D. W., *Surf. Sci.*, 53, 74, 1975; Tice, D. R., *Surf. Sci.*, 40, 499, 1973.
63. Graham, W. R. and Ehrlich, G., *J. Phys. F,* 4, L212, 1974.
64. Slater, J. C. and Koster, G. F., *Phys. Rev.*, 94, 1498, 1954.
65. Pettifor, D. G., *J. Phys. C,* 2, 1051, 1969.
66. Hodges, L., Ehrenreich, H., and Lang, N. D., *Phys. Rev.*, 152, 505, 1966; Mueller, F. M., *Phys. Rev.*, 153, 659, 1967; Heine, V., *Phys. Rev.*, 153, 673, 1967.
67. Haydock, R., Heine, V., and Kelly, M. J., *J. Phys. C,* 5, 2845, 1972; 8, 2591, 1975; Haydock, R. and Kelly, M. J., *Surf. Sci.*, 38, 139, 1973.
68. Cunningham, S. L., Dobrzynski, L., and Maradudin, A. A., *Phys. Rev. B,* 7, 4643, 1973; *Vide,* 28, 171, 1973.
69. Schick, M. and Campbell, C. E., *Phys. Rev. A,* 2, 1591, 1970.
70. Lau, K. H. and Kohn, W., *Surf. Sci.*, 65, 607, 1977.
71. Einstein, T. L., unpublished.
72. Einstein, T. L., *Phys. Rev. B,* 16, 3411, 1977.
73. Einstein, T. L., *Bull. Am. Phys. Soc.*, 21, 304, 1976; Proc. 35th Annu. Conf. Physical Electronics, Pennsylvania State University, University Park, 1975.
74. Glasser, M. L. and Bagchi, A., *Prog. Surf. Sci.*, 7, 113, 1976.
75. Liebsch, A., *Phys. Rev. Lett.*, 32, 1203, 1974; *Phys. Rev. B,* 13, 544, 1976; Solid State Commun., 19, 1193, 1976.
76. Liebsch, A., *Phys. Rev. Lett.*, 38, 248, 1977.
77. Davenport, J. W., *Phys. Rev. Lett.*, 36, 945, 1976; *Bull. Am. Phys. Soc.*, 22, 313, 1977; Ph.D. thesis, University of Pennsylvania, Philadelphia, 1976.
78. Gomer, R., *CRC Crit. Rev. Solid State Mat. Sci.*, in press.
79. Cohen, P. I., Unguris, J., and Webb, M. B., *Surf. Sci.*, 58, 429, 1976; Bruch, L. W., Cohen, P. I., and Webb, M. B., *Surf. Sci.*, 59, 1, 1976; Webb, M. B. and Cohen, P. I., *CRC Crit. Rev. Solid State Sci.*, 6(3), 253, 1976.
80. Huang, K., *Statistical Mechanics,* John Wiley & Sons, New York, 1967, 329.
81. Binder, K. and Landau, D. P., *Surf. Sci.*, 61, 577, 1976.
82. Doyen, G., Ertl, G., and Plancher, M., *J. Chem. Phys.*, 62, 2957, 1975.
83. Somorjai, G. A. and Szalkowski, F. Z., *J. Chem. Phys.*, 54, 389, 1971.
84. Fan, C. and Wu, F. Y., *Phys. Rev.*, 179, 560, 1969; for $E_1 > |E_2|$, T_c is accurate to within a few percent.
85. Estrup, P. J., in *The Structure and Chemistry of Solid Surfaces,* Somorjai, G., Ed., John Wiley & Sons, New York, 1969, 19.
86. Buchholz, J. C. and Lagally, M. G., *Phys. Rev. Lett.*, 35, 442, 1975.
87. Lu, T. M., Wang, G. C., and Lagally, M. G., *Phys. Rev. Lett.*, 39, 411, 1977.
88. Guinier, A., *X-Ray Diffraction,* W. H. Freeman, San Francisco, 1963, 129.
89. Gomer, R., *Solid State Phys.*, 30, 93, 1975.
90. Estrup, P. J., *Phys. Today,* 28(4), 33, 1975; Huang, C. H., Ph.D. thesis, Brown University, 1974.
91. Felter, T. E., Barker, R. A., and Estrup, P. J., *Phys. Rev. Lett.*, 38, 1138, 1977.
92. Einstein, T. L., in Proc. 37th Annu. Conf. Physical Electronics, Stanford, June 20 to 22, 1977; *Surf. Sci.*, to be published.
93. Burton, W. K., Cabrera, N., and Frank, F. C., *Philos. Trans. R. Soc.*, 243, 299, 1951.
94. von Laue, M., *Z. Kristallogr.*, 105, 124, 1943.
95. Herring, C., in *Structure and Properties of Solid Surfaces,* Gomer, R. and Smith, C. S., Eds., University of Chicago Press, Chicago, 1953, 5.
96. Roelofs, L. D., and Einstein, T. L., unpublished; see also Roelofs, L. D., Park, R. L., and Einstein, T. L., *J. Vac. Sci. Tech.*, to be published.
97. Sommerfeld, A., *Optics,* Academic Press, New York, 1954, 234.
98. Herring, C., *Phys. Rev.*, 82, 87, 1951.
99. Park, R. L., Houston, J. E., and Schreiner, D. G., *Rev. Sci. Instrum.*, 42, 60, 1971.
100. Park, R. L., in *The Structure and Chemistry of Solid Surfaces,* Somorjai, G. A., Ed., John Wiley & Sons, New York, 1969, 28; Houston, J. E. and Park, R. L., *Surf. Sci.*, 21, 209, 1970.

101. **Kunz, A. B., Guse, M. P., and Blint, R. J.,** *J. Phys. B,* 8, L358, 1975; **Blint, R. J., Kunz, A. B., and Guse, M. P.,** *Chem. Phys. Lett.,* 36, 191, 1975.
102. **Johnson, K. H.,** *CRC Crit. Rev. Solid State Mat. Sci.,* in press.
103. **Cowan, P. L. and Tsong, T. T.,** in Proc. 37th Annu. Conf. Physical Electronics, Stanford University, June 20 to 22, 1977; *Surf. Sci.,* to be published; **Tsong, T. T.,** *CRC Crit. Rev. Solid State Mat. Sci.,* 7(2), 1978.
104. **Tamm, P. W. and Schmidt, L. D.,** *J. Chem. Phys.,* 51, 5352, 1979; **Tracy, J. C.,** *J. Chem. Phys.,* 56, 2736, 1972; **Tracy, J. C. and Burkstrand, J. M.,** *CRC Crit. Rev. Solid State Mat. Sci.,* 4, 381, 1974.
105. **Latanision, R. M.,** *CRC Crit. Rev. Solid State Mat. Sci.,* 7(3), 1978.
106. **Stern, E. A.,** in *Physics of Solid Solution Strengthening in Alloys,* Plenum Press, New York, 1973.
107. **Blakely, J. M.,** *CRC Crit. Rev. Solid State Mat. Sci.,* in press.
108. **Lau, K. H. and Kohn, W.,** *Surf. Sci.,* 75, 69, 1978.
109. **Rudnick, J.,** *Phys. Rev. B,* 5, 2863, 1972.
110. **Lighthill, M. J.,** *Introduction to Fourier Analysis and Generalized Functions,* Cambridge University Press, Cambridge, 1958.
111. **Schrieffer, J. R. and Wolff, P. A.,** *Phys. Rev.,* 149, 491, 1966.
112. **Einstein, T. L.,** *Surf. Sci.,* 75, 161L, 1978. **Roelofs, L. D. and Einstein, T. L.,** *Bull. Am. Phys. Soc.,* 23, 362, 1978.
113. **Caroli, B.,** *J. Phys. Chem. Solids,* 28, 1427, 1967.
114. Since a vector connecting a site in the top layer with *any* site in the second layer can serve as τ, there are a myriad of critical directions. Moreover, recent unpublished calculations by Lau, K. H. and Kohn, W. suggest that R^{-5} behavior holds in *all* directions.
115. **Grimley, T. B. and Rosales Medina, M. A.,** have performed a similar computation for the c(2 × 2) overlayer using a finer grid, while there are some minor changes (of order 10%) in some peak heights, the qualitative (and semiquantitative) features are largely the same, private communication.
116. The author has recently received preprints discussing specific systems from unorthodox viewpoints. Gallagher, J. M., Haydock, R., and Heine, V., describes the ordered overlayers of O/Ni(100) on the basis of van der Waals attractions between extended local orbitals of oxygen anions. Theodorou, G., treats O/W(110) from a local molecular-like distortion picture.
117. **Ching, W.-Y., Huber, D. L., Lagally, M. G., and Wang, G,-C.,** *Surf. Sci.,* 77, 550, 1978, have shown how trio repulsions of a certain minimum strength can explain the marked asymmetrics in the phase diagram of O/W(110). Explicit model calculations by Einstein, T. L., Proc. 38th Annu. Conf. Physical Electronics, Gatlinburg, June 19 to 21, 1978, submitted to *Surf. Sci.,* explore the hierarchy of trio interactions, find that the strengths required by Ching et al. can exist, but suggest that more configurations contribute comparably, thereby lowering the minimum repulsion.
118. More generally, the calculation of the asymptotic form of G_{oo} turns out to be essentially a two-dimensional case of Koster, G. F., *Phys. Rev.,* 95, 1436, 1954. In equation 27, the appropriate k is that point on the curve of constant ε at which the *velocity* parallels R_n. The vanishing in the <10> case is due to cancellation of contributions from two "sheets" of constant ε. Roelofs, L. D. and Einstein, T. L., unpublished.